REFERENCE CROP EVAPOTRANSPIRATION ESTIMATION USING REMOTE SENSING TECHNIQUE

A dissertation

Submitted in partial fulfillment of the

Requirements for the award of the degree

Of

MASTER OF TECHNOLOGY

IN

IRRIGATION WATER MANAGEMENT

BY

SAMUEL MALOU MUKPUOU DOHL

(Enroll. No: 16547010)

DEPARTMENT OF WATER RESOURCES DEVELOPMENT AND MANAGEMENT

INDIAN INSTITUE OF TECHNOLOGY ROORKEE

ROORKEE-247667, UTTARAKHAND (INDIA)

May, 2018

CANDIDATE'S DECLARATION

I hereby certify that the work presented in this dissertation entitled, "**REFERENCE CROP EVAPOTRANSPIRATION ESTIMATION USING REMOTE SENSING TECHNIQUE**" in partial fulfillment of the requirements for the award of degree of **Master of Technology in Irrigation Water Management** submitted in the Department of Water Resources Development and Management, Indian Institute of Technology Roorkee, Roorkee, is a true record of my own work carried out during the period from July 2017 to May 2018 under the supervision of **Dr. Ashish Pandey**, Associate Professor, Department of Water Resources Development and Management, Indian Institute of Technology Roorkee, Roorkee, and **Dr. V.M Chowdary**, Scientist/Engg 'SG' RRSC-N, NRSC, ISRO; Dos Branch secretariat Loknayak Bhawan Gate 1, Wing A, 3rd Floor Khan Market-New Delhi.

The material presented in this dissertation has never been submitted by me for award of any other degree.

Place: Roorkee

Dated: May, 2018 (**SAMUEL MALOU MUKPUOU)**

This is to certify that the above statement made by the candidate is correct to the best of our knowledge.

(Dr. V.M Chowdary)
Scientist/Engg 'SG'
RRSC-N, NRSC, ISRO; Dos Branch secretariat
Loknayak Bhawan
Gate 1, Wing A, 3rd Floor
Khan Market-New Delhi

(**Dr. Ashish Pandey**)
Associate Professor
Department of Water Resources
Development and Management
Indian Institute of Technology Roorkee
Roorkee – 247 667, Uttarakhand (INDIA)

ACKNOWLEDGEMENTS

First and foremost I thank Almighty God, because without His blessings this work would have been impossible.

I am thankful to Dr. Ashish Pandey, Associate Professor, Department of Water Resources Development & Management, Indian Institute of Technology Roorkee and Dr. V.M Chowdary, Scientist/Engg 'SG' RRSC-N, NRSC, ISRO; Dos Branch secretariat-New Delhi, who besides being my supervisors, tirelessly worked hard to ensure that I managed to complete this study. Their commitment all throughout my studies was overwhelming.

I wish to express my sincere gratitude to Prof. S.K Mishra, Head, Department of WRD&M, IIT Roorkee and staff of the Department of WRD&M, IIT Roorkee for their support and imparting knowledge with care and affection throughout the time of studies. Thanks also to WRD&M's PhD scholars for their tremendous help in the course of this work.

Special thanks to the Indian government for financially supporting this studies through Indian Technical and Economic Cooperation (ITEC) scholarship scheme.

Thanks to University of Juba's management, for granting me the opportunity to pursue the studies. Special thanks to Dr. James Janthana, Dean, College of Engineering and architecture, university of Juba and Dr. El-Khamil Hamad, Head Department of Agricultural Engineering, university of Juba, for their backing and inspiration in my academic endeavor.

I would also like to thank Juba International Airport Authority for providing me with the weather data for accomplishing this research.

Last but not least I will never forget to thank my immediate family members who understood the need for me to be away for studies, their patience and encouragements energized me more in this work.

ABSTRACT

Reference crop evapotranspiration (ETo) is an important element for irrigation water management and its estimation is crucial. Many empirical and physical based approaches have been developed over the years for its estimation. However, lack of conventional ground weather station data, required by these approaches is a big challenge in a developing country like South Sudan, Eastern Africa, whose population depend mainly on rain-fed agriculture whose production diminished tremendously in recent years. Irrigation is being taken up as a remedy for diminished food production but due to non-availability of data for reference crop evapotranspiration, irrigation planning and management is seriously affected. Thus, this study proposes simple remote sensing technique for estimating monthly reference crop evapotranspiration without ground weather station data, using high spatial resolution remote sensing data, in dry season of South Sudan. The study evaluated the use of land surface temperature retrieved from Landsat 8 data as an alternative input for seven commonly used temperature based models (Blaney-criddle, Thornthwaite, Hargreaves (1985), Trajkovic (2007) modified Hargreaves, Droogers et al. (2002) modified Hargreaves, Allen (1993) modified Hargreaves and Kharrufa models) in Juba county of South Sudan. The proposed methodology has also been compared with analogous procedure proposed by Maeda et al. (2011) that use moderate resolution imaging spectroradiometer (MODIS) land surface temperature. Further, the study also proposes the automatic satellite image processing algorithms for each of the temperature based ET_o methods for simplicity of images processing and calculations involve. For broader analysis, the proposed methodology was also tested in Roorkee region, India. The evaluation of the modelled results with FAO Penman Montieth results (using station data) as reference, shows that the models parameterized with Landsat 8 LST performed better than MODIS based, with low RMSE and MAE that ranges from 0.1064 to 0.1165mm/day and 0.0163 to 0.0997 mm/day respectively and high coefficients of determination (R^2) of above 0.9. Hargreaves (1985) method was the best of all, in the study area (Juba County), with overall RMSE of 0.1064 mm/day, MAE of 0.0163mm/day and coefficient of determination (R^2) of 0.93. ET_o maps of study area (Juba County) were prepared using selected method (Hargreaves (1985). So considering the lack of ground station data for ET_o estimation in the study area, the proposed methodology in this study may be used for monthly ET_o estimation and will be of great help in planning, design and management of irrigation systems as well as other water management activities

TABLE OF CONTENTS

LIST OF TABLES

LIST OF FIGURES

LIST OF IMPORTANT SHORTFORMS/ACRONYMS

A_L/Rad_ADD	Band-specific additive rescaling factor
ASTER	Advanced Space borne Thermal Emission and Reflection Radiometer
AVHRR	Advanced very-high-resolution radiometer
BT	Brightness temperature
CFSR	Climate Forecast System Reanalysis
DNs	Digital numbers
DTM	Digital Terrain Model
ETo	Reference crop evapotranspiration
FAO-PM	Food and Agriculture Organization-Penman montieth Method
GIS	geographic Information system
GOSS IDMP	government of south Sudan, Irrigation development master plan
Kc	Crop coefficient
LPDAAC	Land Processes Distributed Active Achieve Center
LSE	Land Surface Emissivity
LST	Land Surface Temperature
Lλ/TOA_RAD	Top of Atmospheric spectral radiance
MAE	Mean Absolute Error
MODIS	MODerate resolution Imaging Spectroradiometer
Moi_LST	Month of interest land surface temperature
NCEP	National Center for Environmental Prediction
NDVI	Normalized Difference Vegetation Index
NOAA	National Oceanic and Atmospheric Administration
OLI & TIRS	Operation Land Imager and Thermal Infrared Sensor
PE	Percentage Error
PV	proportion of vegetation
Ra	Extraterrestrial radiation
Rad_MULT /M_L	band-specific multiplicative rescaling factor
REEM	Regional ET Estimation Model
Ref_ADD	band's reflectance additive rescaling factor
Ref_MULT	band's reflectance multiplicative rescaling factor
RMSE	Root Mean Squared Error
SEBAL	Surface Energy Balance Algorithm for Land
S-SEBI	simplified-Surface Energy Balance Index
TDR	Time-Domain Reflectometer
TOA_Ref	Top Of Atmosphere Reflectance
USGS	United States Geological Survey
UTM	Universal Transverse Mercator
VITT	Vegetation Index/Temperature Trapezoid

CHAPTER I

INTRODUCTION

1.1 BACKGROUND

Water is a crucial asset for all forms of life on this earth. It is used for agriculture and many other purposes. In the current world, the demand for water is increasing day by day as a direct consequence of ever growing population and rapid industrialization and urbanization. Thus, stiff competition exists among different water consuming sectors. Wisser et al., (2008) indicated that 70% of the global water consumption accounts for agricultural production. However, this agriculture consumption varies from country to country depending on the priority of the sector in the respective country.

Need to increase food availability for meeting the needs of ever increasing population globally, further exerts enormous pressure over this scarce and precious resource (water). Hence, available water share for agriculture has to be managed optimally, as agricultural sector faces tough competition with other stakeholders.

One basic parameter in irrigation management as well as other water management activities is reference crop evapotranspiration (ET_o). ET_o indicates the water lost through evaporation and transpiration from hypothetical grass surface, not short of moisture (Allen et al. 1998), its represents the evaporation power of a place's atmosphere. And its estimation is of great value in planning, design and management of irrigation systems (Droogers & Allen, 2002; Kisi, 2013; Valipour, 2015; Trajkovic, 2005; Azhar & Perera, 2011; Bajirao & Awari, 2017)

Data on reference crop evapotranspiration (ETo) helps in knowing crop water requirement (CWR) (CWR is the water needed to compensate the water lost through evapotranspiration) (Efthimiou et al. 2013). And so, it's of paramount importance in agricultural studies(Sarangi & Parihar, 2016)

Direct measurement of ET_o is quite difficult; labor intensive, time consuming and costly and hence, indirect methods of estimating ET_o from meteorological data remain a substitute (Rao, Sandeep, & Venkateswarlu, 2012). However, input datasets for climatological ET_o methods is a problem in south Sudan as well as other developing countries.

1.2 PROBLEM STATEMENT

Several models for computing ET_o from climatological data have been developed over the years, and these models differ in term of input data. Some need more and some need less data. The input data conventionally, is obtain from established weather stations over the area of interest. However, creation and maintenance of agro-meteorological stations capable of gauging such parameters is very difficult and costly, even simple, easily measured parameter like air temperature measurement may be impossible at some places of concern. Example of such places is south Sudan, in East Africa, where only five (5) weather stations out twenty nine (29) that were set up are functional (GOSS IDMP Report, 2015)

Generally, in most of the developing countries, meteorological stations are often inadequate to acquire the information required to signify the spatial and temporal variation of ET_o and as such irrigation water management as well as water resources management in general, is often affected in such information deficit areas.

Thus, concentrated efforts are essential to search for alternative approaches and datasets to be used in developing countries that are highly affected by hunger and water scarcity. And the blend of ET models with remote sensing data provides a possible substitute to obtain temporally and spatially constant information about land surface processes like evapotranspiration. It has been indicated that, in poorly gauged basins, remote sensing data can significantly improve the availability of necessary information, for example albedo, leaf area index and Land Surface Temperature (Wagner, 2008; Wagner et al. 2009).

In the run of closing the meteorological data gap for ET_o estimation, the current study examined the use of satellite land surface temperature, on high spatial resolution, as input, instead of traditional air temperature, for seven ET_o, temperature-based models in south Sudan-Juba County, one of the regions of great value in terms of irrigated agriculture

1.3 REMOTE SENSING AND GIS TECHNIQUE

Remote sensing means acquiring information about an object, from a remote platform, by utilizing the properties of electromagnetic wave emitted, reflected or diffracted by the sensed object. Thus, Remote sensing technique is used for getting information about the earth surface features for the purpose of enhancing natural resources management i.e. water management. While Geographic Information System (GIS) is a collection of computer hardware and software, data and skilled

personnel for managing and analyzing geographic data. In this study the techniques are mainly employed to derive and analyze spatial data input for temperature-based ET_o methods.

1.4 JUSTIFICATION AND MOTIVATION

This study proposes to utilize remote sensing and GIS technique, in irrigation water management in South Sudan-Juba County. Due to water scarcity, population growth and limited water resources, government and private sectors are putting priority on resolving this problems. The main water management problems of the study area include:

a) Lack of fundamental agro-climatic data" for planners and decision makers
b) Lack of idea in managing water supply and demand for agriculture
c) Limited application of remote sensing and GIS techniques in water resources management.

Hence, the significance of this study can be enumerated as follows:

a) It illustrate the use of remote sensing and GIS tools in giving solution for water management problems, through estimation of reference crop ET.
b) Provide new technique for ET_o estimation in the study area and will be of great help to decision makers.
c) It is first study in South Sudan Juba County to provide ET_o maps on high spatial resolution
d) The procedures are simple to follow and hence it's efficient way of computing ET_o

1.5 SCOPE AND OBJECTIVES

The current study evaluates the use of remotely sensed land surface temperature (LST) on high spatial resolution (Landsat 8 LST) as an alternative input for seven temperature based ET_o methods in Juba County, South Sudan and comparison of the proposed methodology with the similar procedure, proposed by (Maeda et al. 2011), which use coarse spatial resolution data (Moderate resolution Imaging Spectroradiometer (MODIS) land surface temperature (LST))

Looking to the aforementioned, the main objective of this study is to estimate the monthly ET_o values employing high spatial resolution remote sensing data and empirical ETo equations, without ground stations data involve. The study also evaluates the same procedure in Roorkee, India for broader analysis.

The specific objectives of this study are as follows:

1. Performance evaluation of seven (7) temperature-based ET_o models; Thornthwaite, Blaney-criddle, Kharrufa (1985), Hargreaves (1985), Droogers et al. (2002) modified Hargreaves,

Allen et al. (1993) modified Hargreaves and Trajkovic (2007) modified Hargreaves methods, when taking satellite remote sensing derived LST as input instead of air temperature

2. Relative evaluation of temperature-based reference evapotranspiration models (ET_o) using satellite remote sensing derived Land surface Temperature (LST)
3. Calibration and validation of the LST based ET_o models for the identified study area(s)
4. Generation of spatially distributed ET_o maps.

1.6 THESIS ORGANIZATION

This thesis is categorized into five chapters as follows:

Chapter 1 presents the introduction which comprises of the research background, statement of problem, motivation, scopes and objectives. Chapter 2 gives information about the previous studies on the research topic and also list the gaps identified in the previous studies. Chapter 3 describes the study locations, input data and methodologies involve. Chapter 4 presents the results and their analysis. Chapter 5 provides the thesis conclusion, limitations and proposed future works

CHAPTER II

LITERATURE REVIEWS

This chapter discusses the review of literature on measurement of ET_o and the past studies on using remote sensing technique for ET estimation

2.1 GENERAL REVIEW ON REFERENCE EVAPOTRANSPIRATION MEASUREMENT

There are several techniques for direct measurement of reference crop evapotranspiration. Rao et al., (2012) showed that measurement of reference evapotranspiration can be done using Water budgeting technique, Direct soil water measurement (like neutron probe, Gravimetric, TDR etc), Hydrologic budget (mass balance) methods, Lysimetric measurement, Bowen ratio, eddy correlation, Chamber techniques, Biological (i.e. Sap flow technique) methods, Pan evaporation method. However, all of the mentioned direct ET measurement techniques are difficult to care out and cost prohibitive in most cases. Furthermore, their estimates represent only point ET values and Liou & Kar, (2014) mention that they can only be used for accurate measurement of homogeneous areas and this is very uncommon case for large fields. Also in different study, Allen et al., (1998) mentioned that direct measurement of evapotranspiration is not easy, it needs special devices, accurate measurements, trained personnel and high investments. Rao et al. (2012) reported that indirect methods that use meteorological data are alternative for ET_o estimation, and they are widely used. Again lack of ground weather station data required by these indirect ET_o approaches is a big drawback for their application in developing countries. Thus, satellite remote sensing application appears to be the substitute modern technique for ET_o and other land processes monitoring. Wagner et al. (2009) reported that satellite remote sensing technique can fill the data gaps in developing countries and (Tsouni et al., 2008) mentioned that satellite remotely sensed data is of paramount importance in assessing evapotranspiration and other meteorological variables. Hence the current study intends to use remote sensing technique to derive input data for some commonly used ET_o models.

2.2 REVIEWS OF LITERATURE ON PAST STUDIES ON THE USE OF SATELLITE REMOTE SENSING DATA IN ET_o ESTIMATION

Interests and efforts in using satellite remote sensing techniques, for obtaining evapotranspiration is not of recent only, many studies had been conducted over the years and sure many, may be on going.

Maeda, Wiberg, & Pellikka, (2011) evaluated MODIS sensor land surface temperature, in temperature based ET models (Thornthwaite, Blaney-Criddle and Hargreaves) in Taita Hills area in Kenya-with the objective of overcoming limited ground meteorological data availability for ET

models. They indicated that consistency exists between satellite derived LST based ET_o and In situ ET_o. Hargreaves method estimates were more reliable in this study with an average RMSE of 0.47 mm/day and a correlation coefficient of 0.67.

El-Shirbeny, (2016) evaluated Hargreaves' model based on remote sensing technique to estimate potential crop evapotranspiration (ET_o) in three regions of Alexandria, El-Minya and Aswan in Egypt. Major inputs for computation of ET_o such as Normalized Difference Vegetation Index (NDVI) and Land Surface Temperature (LST) were derived from NOAA/AVHRR and Landsat 8 satellite data. Further satellite LST based ET_o were compared with ground based ET_o estimates by FAO Penman-Monteith (FAO-PM) and Hargreaves methods and found to have strong correlation as high as 0.99..

Ray & Dadhwal, (2001) estimated seasonal crop evapotranspiration in Mahi Right Bank Canal command area of Gujarat, India using both remote sensing and meteorological observations. IRS-1C WiFS (Wide Field Sensor) satellite data was used for generation of land use/cover and crop coefficient maps. This study used crop coefficients (Kc) derived from NDVI and found that ET_c estimate with RS data was more promising.

Tran & Pinon, (2009) assessed ET variation in pecan fields of lower Rio Grande Valley in New Mexico using one of the energy balance model i.e. Regional ET Estimation Model (REEM). Remote sensing based ET estimates were found to be compared realistically well with actual eddy covariance system values in a matured pecan orchard with an average error of 4% and the standard error of estimate (SEE) ranging from 0.91 to 1.06 mm/day.

Bois et al., (2008) investigated the use of solar radiation derived from Meteosat satellite images using Heliosat-2 method, for estimation of daily evapotranspiration by radiation-based and FAO Penman-Montieth methods, in Southern France. They reported that solar radiation values from HelioClim-1 database are lower by 14-20% of the stations' mean annual values. However uncertainties of this data was found to be small in FAO PM Methods and was generally suggested that satellite sensed solar radiation may improve evapotranspiration estimation in places where air temperature is available.

Kamble, Kilic, & Hubbard, (2013) developed a simple linear regression equation for calculating crop coefficient from Normalized Difference Vegetation Index (NDVI), in high plains of USA. They

reported that good linear correlation exists between remote sensing Kc based on NDVI and measured Kc, with root mean square error of 0.16 and 0.19 for 2006 and 2007 respectively.

Lanjeri et al. (2007) used Digital Terrain Model (DTM) and GIS technique to estimate the extraterrestrial radiation parameter (Ra) in Hargreaves ET method and compared the results with latitude corrected Ra, in the northernmost semi-arid region of Europe, the Ebro valley. They reported that the DTM and GIS estimated Ra was better than latitude estimated Ra.

Papadavid et al. (2011) incorporated remotely sensed data from MODIS-TERRA and Landsat TM and TM+ in FAO Penman-Monteith ETc method in order to evaluate the effect of reduced for ETc computations in Cyprus. They reported that satellite based ET_c is under estimated as compared to meteorological station data and found that the difference was said to be insignificant.

Li et al. (2008) computed crop evapotranspiration (ETc) for wheat crop using SEBAL model while Hargreaves method was used for reference evapotranspiration (ETo). It was reported that the daily ET estimates from SEBAL model are in good agreement with the Lysimeter data. The error of ET estimation over the whole growing stage of winter wheat was roughly 4.3%.

Weligepolage, (2005) compared remote sensing methods (SEBAL and S-SEBI) with traditional ground based methods for estimation of the actual evapotranspiration in HupselseBeek catchment in the Netherlands. SEBAL & S-SEBI estimates were found to be well distributed spatially.

Tasumi et al. (2003) reported that the, SEBAL based ET estimates matched well with lysimeter based ET estimates for agricultural crops in the semi-arid climate of western USA

Yang, Zhou, & Melville, (1997) used Vegetation Index/Temperature Trapezoid (VITT) concept for estimation of evapotranspiration using land surface temperature and NDVI derived from Landsat Thematic Mapper (TM) data for sugarcane fields of Northern New South Wales in Australia. They concluded that ET estimation through this approach can be a better alternative for sugarcane fields at local scale.

Granger, (2000) estimated evapotranspiration in the Gediz basin, Turkey using NOAA-AVHRR and LANDSAT images.

(R. Li, Min, & Lin, 2018) employed remote sensing data (emissivity different vegetation index) from special sensors microwave imager (SSM/I) to estimate evapotranspiration of Harvard forest, USA

Zheng & Zhu, (2015) evaluated Thornthwaite and Hargreaves methods in North China, using land surface temperature and Normalized Difference Vegetation Index obtained from moderate resolution imaging spectroradiometer (MODIS) sensor data

Montes et al. (2017) used remote sensing technique to estimate the daily ET in vineyard field in Languedoc-Roussillon, Southern France. They used ASTER and ETM+ data as input for Simplified Surface Energy Balance Index (S-SEBI) method.

Tsouni et al.,(2008) evaluated the application of remote sensing data from NOAA-AVHRR in combination with station measured data to estimate the actual daily ET over Thessaly plain, Greece. They found that remote sensing data can help a lot in assessing actual evapotranspiration and other meteorological variables in places with limited ground station networks.

Several researchers reported that the estimation of evapotranspiration using remote sensing data or approaches is quite promising and is a viable alternative for conventional approaches. Limited studies are carried out for relative evaluation of satellite based temperature based ET estimates

2.3 RESEARCH GAPS

1. Some of the ET approaches require large data, which often limit their use due to lack of ground station data.
2. Very few studies are carried out to test the use of LST derived from Landsat 8 and MODIS images as alternative input for air temperature while computing ET.
3. Satellite image processing models for automatic generation of evapotranspiration by temperature-based methods, inputting LST of Landsat 8 data, have never been given attention in the past studies.

CHAPTER III

MATERIAL AND METHODS

This chapter entails the description of the study area, climatological methods for estimation of ET_o, input data and the methodology followed.

3.1.0 STUDY AREA DESCRIPTION

The study has been conducted for two locations namely Juba County located in South Sudan, East Africa and Roorkee, located in Northern India.

3.1.1 Study Location 1

The study area, Juba County is situated in South Sudan, the newest nation in Africa that became independent from Sudan on July 9th 2011. It is a landlocked country, bounded on the north by Sudan, on the west by central Africa Republic, Democratic Republic of Congo on southwest, Uganda on the south, Kenya on southeast and Ethiopia on the east. Geographically, it is situated in the tropical region between Latitudes 3^0N and 13ºN and Longitudes 24ºE and 36ºE and cover nearly 647,000 sq.km geographical area (Figure 3.1). South Sudan is divided into six agro climatic zones namely flood plains, greenbelt, iron stone plateau, Hills and Mountains, Nile and Sobat and Arid (Tizikara, George, & Lugor, 2015) (Figure 3.1). Major occupation in this country is agriculture, which is mostly rainfed. Rainfall distribution in this area is erratic in nature. This made farmers and government to devise strategies for protective irrigation as dry season prevails for almost six months. The weather data used in this study was collected from Juba international airport station, situated at approximately 4.86^0N latitute and 31.6^0E longitute, represnetative of flood plains agro-climatic zone (figure 3.1). Flood Plains is the biggest agro-climatic zone in south sudan. The station is in Juba county and is situated between Latitute of $3^057'26.82''$ N and $5^027'45''$N and Longitude of $30^030'25''$E and $32^013''22.6''$E. covering an area of nearly 18789 sq.km.

South Sudan climate is mostly sub-humid and annual rainfall ranges from 700 mm to 2200 mm with a mean annual rainfall of 900mm. Rainfall distribution in the study area exhibits unimodel and bimodal distributions. Major portion of the study area has unimodal rainfall pattern with wet season from May to October and dry season from November to April. The length of growing period in places with unimodal rainfall is short that ranges from 130 to 150 days annually. Bimodal pattern exists only in greenbelt region and wet season is long starting from April to June. This is often punctuated by bit of dry period during July and rains from August to November. The length of growing period in bimodal region is long that ranges from 280 to 300 days per year.

The average yearly temperatures in south Sudan commonly varies from 25ºC to above 35ºC. According to (FAO Aquastat, 2015) potential evapotranspiration varies from 1400 mm in the southern part to 2400 mm in the northern part annually.

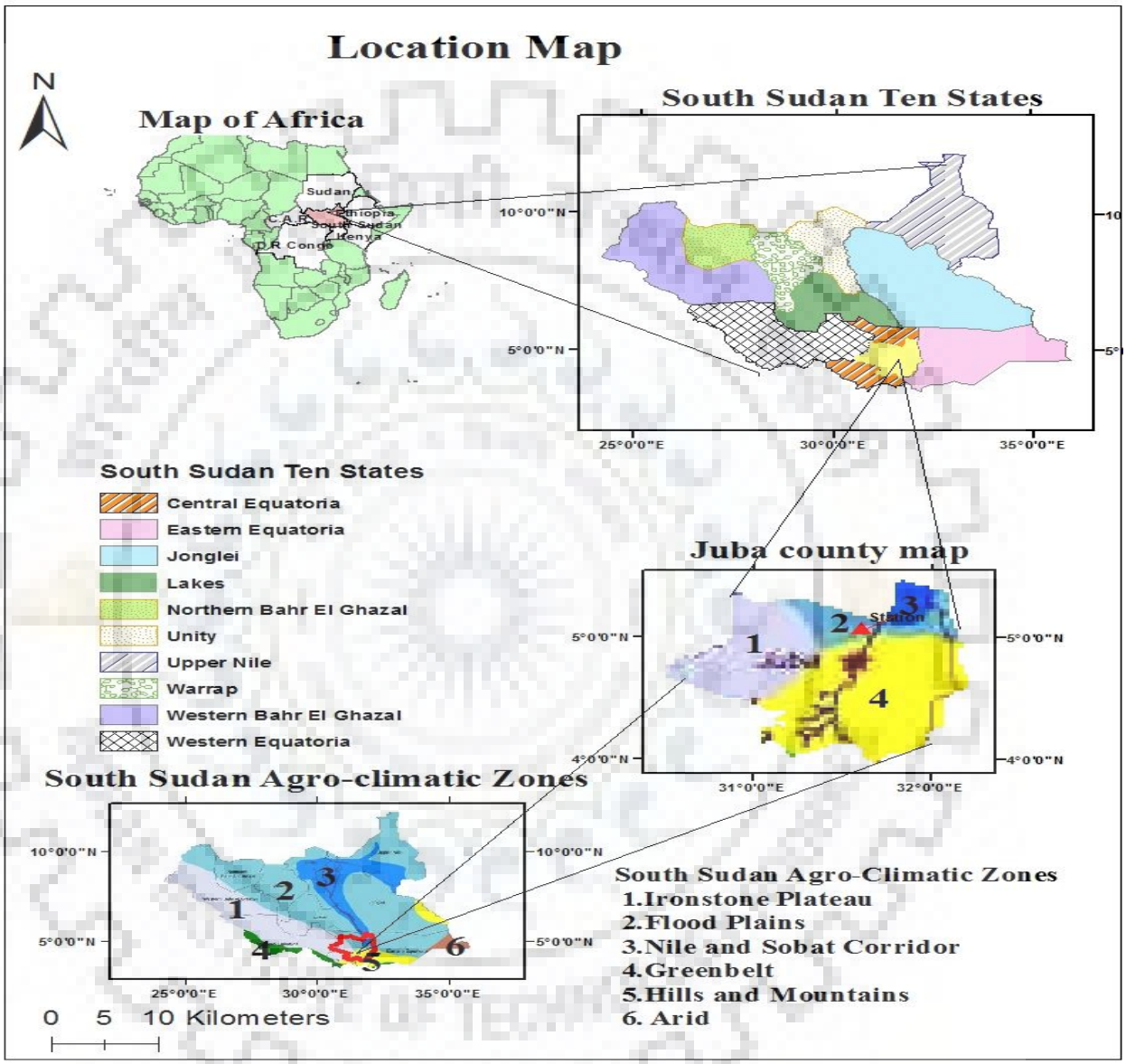

Figure 3. 1 Juba County, Location map

3.1.2 Study Location 2

The study area, Roorkee is in Haridwar district of Uttarakand state, Northern part of India. It is located approximately between $30^0$15'3''N and 29^0 32' 45''N latitudes and 77^0 42' 7''E and 78 6' 33''E longitudes (figure 3.2) and spread over an area of about 1187.2 km^2, on an average elevation of 268 m and distance of about 165km from Dehli and lies between rivers Ganges and Yamuna, near

the foot of Himalayas. It's in warm and temperate climate with average annual temperature of 23.7^{0}C and average annual rainfall of 1170mm (https://en.wikipedia.org/wiki/Roorkee)

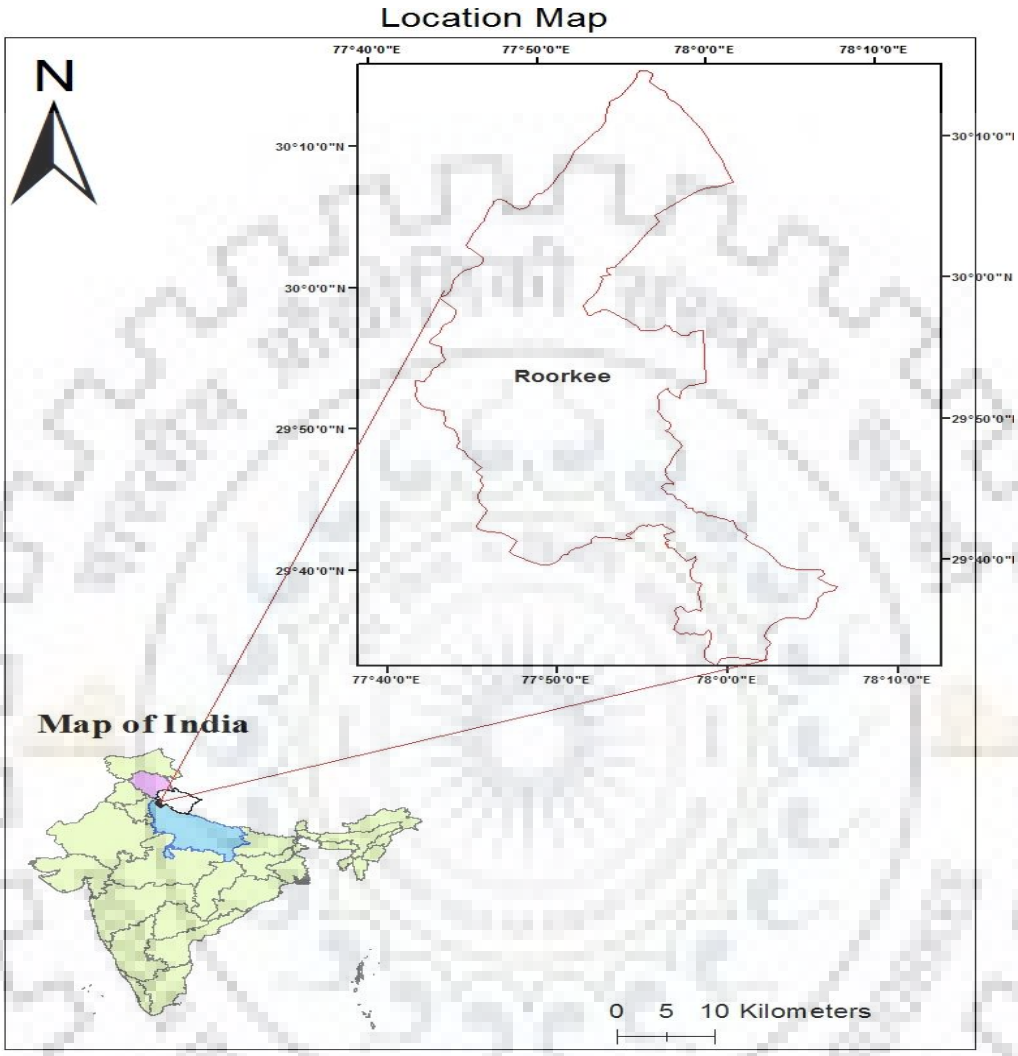

Figure 3. 2:Roorkee, Location map

3.2 CLIMATOLOGICAL ET_O METHODS

Several empirical and physical based climatological ET_o models exist and these models differ in complexity and data requirements. The complex ones need more climatological data and results in good performance for variety of climates while models with limited data are applicable for specific climatic regions. Particularly, availability of climatic data required by the models is difficult for developing country like South Sudan. Even simple air temperature data that is required by temperature based ET_o methods may at some point be very difficult to obtain in south Sudan. In order to overcome data problem, temperature based empirical ET_o models were evaluated by replacing the air temperature with satellite derived LST for ET_o computations. Details of the temperature based models are presented below:

3.2.1 Blaney-Criddle method

Blaney-Criddle ET method is based on the mean air temperature and monthly percentage of day light hours of the period under consideration. Its' modified version is expressed as (Doorenbos & Pruitt, 1977):

$ET_o = p\,(0.46T + 8)$……. (1)

Where ET_o is reference evapotranspiration, mm/day, T is average daily temperature, ^oC, p daylight percent.

3.2.2 Thornthwaite method

Thornthwaite (1948) related a reference crop evapotranspiration with average monthly temperature as (Subedi & Chávez, 2015):

$ET_o = 16(10T/I)^a$ ……(2)

Where ET_o is reference evapotranspiration of standard month of 30 days and 12 hours in mm/month, T is the mean monthly temperature in ^oC, I is the annual thermal/heat index i.e sum of monthly heat index ($i= (T/5)^{1.514}$) and **a** is constant which depend on annual heat index and is expressed as: $a = 6.75x10^{-7}\, I^3 – 7.71x10^{-5}\, I^2 + 1.792x10^{-2}\, I + 0.49239$.

3.2.3 Kharrufa method:

Kharrufa (1985) developed a relationship of potential evapotranspiration with percent of daylight hours and mean monthly temperature. The equation is as follows(Heydari et al. 2014):

$ET_o = 0.34pT^{1.3}$……...(3)

3.2.4 Hargreaves method

Hargreaves and Samani (1985) equation for computing reference evapotranspiration from air temperature is given as below (Hosseinzadeh Talaee, 2014)

$ET_o = 0.0023xR_a\,(T_{mean} + 17.8)(T_{max} – T_{min})^{0.5}$……(4)

Where ETo is reference evapotranspiration in mm/day, R_a is extraterrestrial radiation in mm/day which can simply be obtained from standard tables available in most literatures, T_{mean} is the average daily temperature, T_{max} and T_{min} are maximum and minimum daily temperature respectively.

Nevertheless, the above, original Hargreaves equation was modified by many researchers and the ones that are considered for this study are as follows:

3.2.5 Allen et al (1993) modification to Hargreaves approach

Allen (1993) modified Hargreaves equation using climwat data of 3200 stations and lysimeter data from Davis, California. It is formulated as given below:

$$ET_o = 0.408x0.0030xRa\ (T_{mean}+ 20)(T_{max} - T_{min})^{0.4} \quad \ldots\ldots(5)$$

3.2.6 Droogers et al. (2002) modification to Hargreaves approach

Droogers et al. (2002) modified Hargreaves method, using IWMI gridded climatic atlas data of the world resulted into the following version

$$ETo = 0.408x0.0025xRa\ (T_{mean} + 16.8)(T_{max} - T_{min})^{0.5} \quad \ldots\ldots(6)$$

3.2.7 Trajkovic (2007) modification to Hargreaves approach

Trajkovic (2007) presented modified Hargreaves equation validated for western Balkans region is given as follows:

$$ETo = 0.0023xRa\ (T_{mean} + 17.8)(T_{max} - T_{min})^{0.424} \quad \ldots\ldots(7)$$

3.3 INPUT DATA

Traditionally, weather data used in the ET_o models is obtain from established ground weather stations. However, in south Sudan as well as in other developing nations, getting such data and establishing weather stations is cumbersome. Even simple recording of air temperature is very difficult.

Thus, in this study, remotely sensed data (satellite land surface temperature) is tested as an alternative input for temperature based ET_o methods. Satellite land surface temperature refer to radiometric temperature emitted from the earth surface observed by a sensor on the satellite platform (Avdan & Jovanovska, 2016). Data from two satellites: one with low spatial resolution (Terra data) and one with high spatial resolution (Landsat 8 data) are applied and evaluated in this study.

3.3.1 Landsat 8 data

Operation Land Imager (OLI) and Thermal Infrared Sensor (TIRS) images, onboard Landsat 8 were used for computing Land Surface Temperature (LST).Further, LST was used to compute reference crop evapotranspiration using temperature-based ETo methods. Landsat 8 imageries were downloaded from United States Geological Survey (USGS) website (https://earthexplorer.usgs.gov/). Landsat 8 acquires data from 11 spectral bands, 9 of which are in shortwave, captures by OLI sensor, with 30m spatial resolution except band 8; panchromatic which have 15m. And two thermals bands (10 & 11), captures by TIRS, with 100m resolution (Landsat 8, data users Handbook,2016). In this study, the bands used were Red band (R), Near Infrared (NIR)

band and one TIR band i.e. 10. R and NIR bands were used for computing Normalized Different Vegetation Index (NDVI), Proportion of Vegetation and Land Surface Emissivity (LSE). Although there are two thermal bands (10 and 11), available in the Landsat 8 images for retrieval of radiometric temperature, use of band 11 is not recommended by USGS due to large calibration uncertainty. Thus, band 10 was used for calculating brightness temperature which in turn was used together with land surface emissivity obtained from R and NIR bands to get actual land surface temperature. Band 10 have spatial resolution of 100 m and is resampled to 30 m in this study. The temporal resolution of Landsat 8 satellite is 16 days. Study location, Juba County is covered by four scenes and a total of 28 images with no or less clouds contamination, representing seven months of two dry seasons were employed in this study. Other study location, Roorkee, India, covered by one scene, a total of 8 images corresponding to two *Rabi* agricultural seasons (Rabi season October to March as by (Garg, 2006)) were used. Acquisition details of the satellite data used in this study for two study locations namely Juba county, South Sudan and Roorkee, India, are presented in Tables 3.1& 3.2 respectively.

Table 3. 1: Landsat Images Acquisition Details, Juba county, South Sudan

	Season 1 (Nov 2014 to Feb 2015)		Season 2 (Nov, 2013 to Feb 2014)	
Path-Row	Acquisition Date	Local solar Time	Acquisition Date	Local solar Time
172-56	30-11-2014	0806	29-12-2013	0807
172-57	30-11-2014	0806	29-12-2013	0807
173-56	05-11-2014	0812	20-12-2013	0813
173-57	05-11-2014	0812	20-12-2013	0813
172-56	16-12-2014	0806	30-01-2014	0806
172-57	16-12-2014	0806	30-01-2014	0806
173-56	23-12-2014	0812	05-01-2014	0813
173-57	23-12-2014	0812	05-01-2014	0813
172-56	17-01-2015	0806	15-02-2014	0806
172-57	17-01-2015	0806	15-02-2014	0806
173-56	08-01-2015	0812	22-02-2014	0812
173-57	08-01-2015	0812	22-02-2014	0812
172-56	02-02-2015	0806		
172-57	02-02-2015	0806		

173-56	09-02-2015	0812		
173-57	09-02-2015	0812		

Table 3. 2: Landsat 8 Images Acquisition details, Roorkee, India

SEASON-1 (Oct. 2013 to march 2014)				
Path-Row	Day	Month	Year	Local solar time
146-39	20	10	2013	0520
	21	11		0520
	07	12		0520
	25	02	2014	0519
	29	03		0518
	SEASON-2 (Oct. 2014 to Dec. 2014)			
Path-Row	Day	Month	Year	Local solar time
146-39	23	10	2014	0518
	24	11		0518
	10	12		0518

Since Landsat 8 satellite acquire data at a time, which may not correspond to maximum, mean or minimum temperature acquisition times, LST values obtained from Landsat 8 were scaled using historical long term maximum, minimum temperatures as per ET_o model needs. For scaling the LST, Climate Forecast System Reanalysis (CFSR) historical temperatures (maximum and minimum) data pertaining to identified gridded stations at: 31^0 33' 45''E Longitude, 4^0 50' 22''N Latitude for Juba county and 77^0 48' 45''E Longitude, 29 49' 4''N Latitude for Roorkee, were obtained from National Center for Environmental Prediction (NCEP) website (https://globalweather.tamu.edu/) were used. Maximum and minimum temperature values from NCEP data corresponding to image acquisition months were averaged month wise for 35 years (1979-2013) and their means were also computed. Then scaling ratios (ratio of CFSR temperatures to Landsat 8 LSTs) were first computed month wise and it was found that ratios variation of different months within a season is relatively small for many months and thus, averages were then used. The scaling ratios are shown in tables 3.3 and 3.4 below, for Juba and Roorkee respectively. Scaling was done for the data pertaining to one season, while other season is used for validation. CFSR data is

available globally on 38 km spatial resolution (Fuka et al., 2013) and has been assessed as reliable data (Dile & Srinivasan, 2014).

Table 3. 3: Scaling of Landsat 8 data based on historical max and min temperatures, Juba County, South Sudan

2014-2015: dry season scaling data (all in degree Celsius except ratios)							
month	max	min	mean	LST	max:LST	Min:LST	mean:LST
Nov.	36	22	29	34	1.05	0.64	0.85
Dec	36	21	28	38	0.95	0.54	0.74
Jan.	37	19	28	35	1.06	0.55	0.81
Feb	39	21	30	37	1.05	0.55	0.80
Average scaling ratio					**1.03**	**0.57**	**0.80**

2013-2014: Rabi season scaling data (all in degree Celsius except ratios)							
month	Max.	min.	mean	LST	max:LST	min:LST	Mean:LST
Oct.	31	14	23	26	1.19	0.54	0.87
Nov.	26	9	18	19	1.38	0.47	0.92
Dec.	24	7	16	19	1.27	0.38	0.83
Feb.	26	8	17	18	1.44	0.45	0.95
Mar.	34	15	25	30	1.15	0.49	0.82
Average scaling ratios					**1.29**	**0.47**	**0.88**

Table 3. 4: Scaling of Landsat 8 data based on historical max and min temperatures, Roorkee, India

NB: Max., Min and Mean are averages of maximum, minimum and mean temperature values respectively, obtained from NCEP data, LST is the land surface temperature obtained from Landsat 8 imagery.

3.3.2 MODIS data

MODIS sensor is onboard of two satellites namely Terra and aqua and provides images in 36 bands. The MODIS land surface temperature was downloaded from Land Processes Distributed Active Achieve Center (LPDAAC) website (https://lpdaac.usgs.gov/data_access/reverb). Its spatial resolution is 1 km and temporal resolution is 1 day to 2 days. In this study, MODIS MOD11A2

product, which gives the average values of clear-sky LSTs during 8-day period (day and night) on 1 km resolution, in sinusoidal grid is used.

The day time LST correspond to one obtained by a sensor approximately between 10:00 am to 12:00pm and night time LST correspond to one obtained by sensor approximately between 22:00pm to 23:00 pm. A total of 138 MODIS images for tile numbers h21v08 that cover Juba County, South Sudan and 184 MODIS images for tile numbers h24v05 & h24v06 in which Roorkee, India fall between them, were downloaded from LPDAAC website for three years; 2013, 2014 & 2015 and two years 2013 and 2014 respectively. Re-projection of images to geographic co-ordinate system (Datum WGS84) was carried out in ENVI 5.3 software. Monthly LST was computed by aggregating 8 day LST images. The LST values originally in kelvin were converted to degree Celsius as per ET_o models requirement. The daytime MODIS LST was taken as maximum temperature and night time LST as minimum temperature and their average as mean temperature for application in ET_o models. It was seen that the variation of MODIS LST from station air temperature is small; less than 5^0C in all months except daytime MODIS LST, which was close to 7^0C in the month of March. The variation of MODIS daytime LST, MODIS nighttime LST and MODIS mean LST from maximum air temperature, minimum air temperature and mean air temperature respectively is shown in figure 3.3 below.

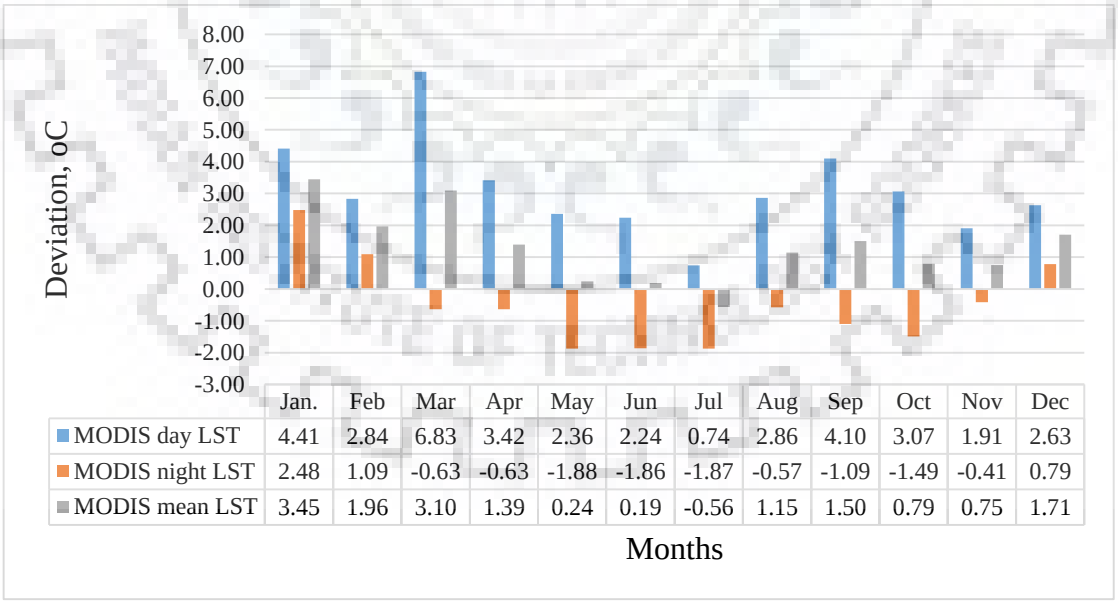

	Jan.	Feb	Mar	Apr	May	Jun	Jul	Aug	Sep	Oct	Nov	Dec
MODIS day LST	4.41	2.84	6.83	3.42	2.36	2.24	0.74	2.86	4.10	3.07	1.91	2.63
MODIS night LST	2.48	1.09	-0.63	-0.63	-1.88	-1.86	-1.87	-0.57	-1.09	-1.49	-0.41	0.79
MODIS mean LST	3.45	1.96	3.10	1.39	0.24	0.19	-0.56	1.15	1.50	0.79	0.75	1.71

Figure 3. 3: Deviation of MODIS LST from Air Temperature (2013 to 2015 deviation of averages)

3.4 METHODOLOGY

3.4.1 Estimation of ET_o from Landsat 8 data

The general framework for computing reference crop evapotranspiration from Landsat 8 data is presented in Figure 3.4 .Initially, null data pixels from the images, downloaded from USGS website, were removed using ArcGIS 10.4. And subsequently these images were mosaicked, subsetted and extracted band wise corresponding to study location in ERDAS IMAGINE 2015. Once the data is acquired, preprocessing of satellite images (bands 4, 5 and 10) are being carried out for retrieval of brightness temperature (BT) and land surface emissivity (LSE). Further, both BT and LSE are used to compute actual land surface temperature (LST), which is scaled to maximum, mean and minimum values using NCEP data as mentioned earlier. The scaled LST is then used for computation of ET_o using temperature based methods.

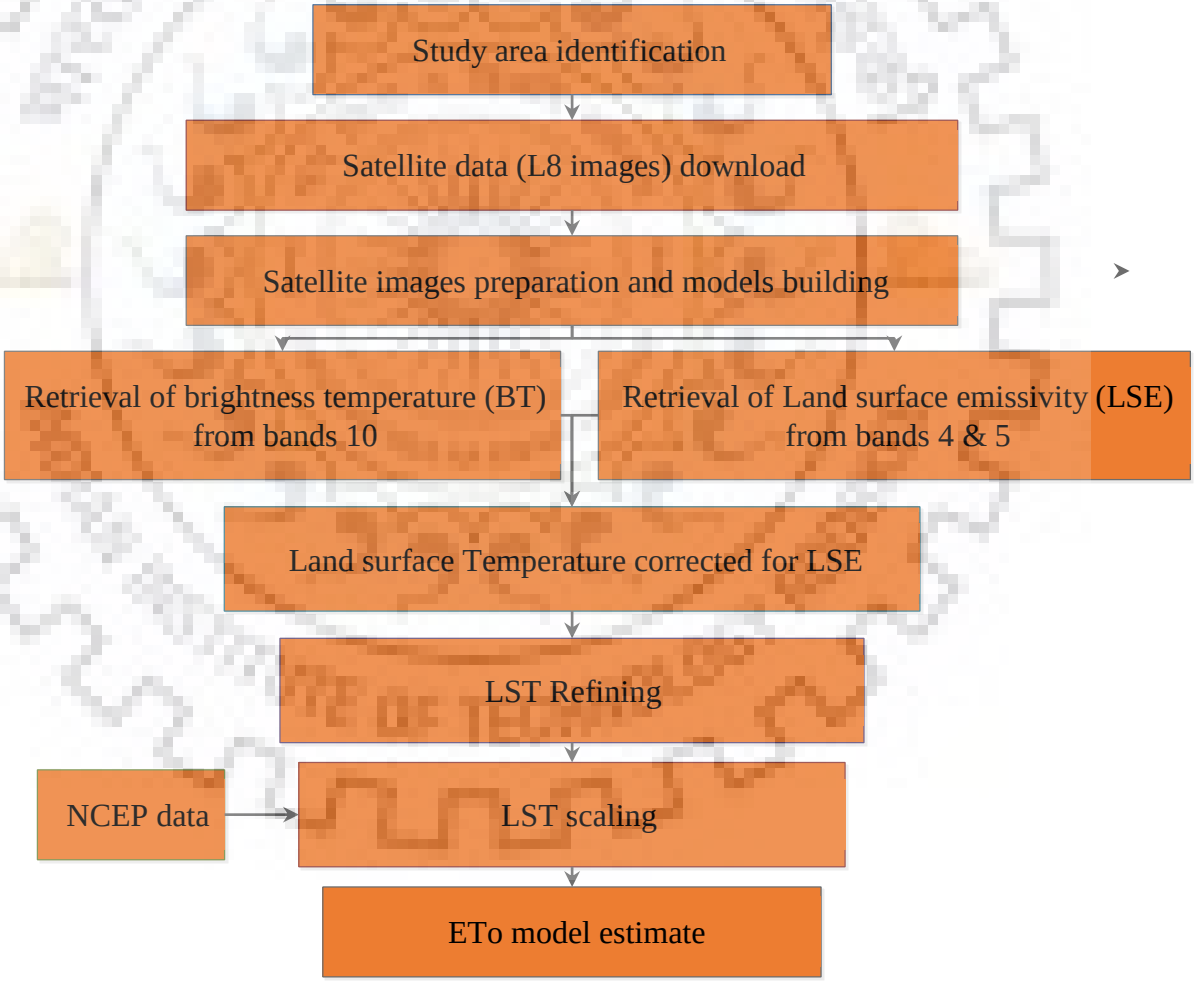

Figure 3. 4:Schematic framework for computation of ETo using satellite derived temperature based methods

3.4.1.1 Specific images processing algorithms

The procedures followed by each of the developed satellite image processing model, based on different ET_o empirical models are discussed below

3.4.1.1.1 Blaney-Criddle ET_o model

The algorithm was developed in ArcGIS 10.4 to derive ET_o from Landsat 8 data. The input data for this model include band 10, NDVI, maximum NDVI and minimum NDVI, satellite images rescaling factors and Blaney-Criddle ET_o equation constant (P). Algorithm uses raster resampling tool to resample band 10, which is originally of 100 m spatial resolution to the same resolution as NDVI i.e.30m and raster calculator tool for all computations. Steps used by the mentioned algorithm for ET_o calculation from Landsat 8 data are presented in figure 3.5 below. With group of steps in the box (GENERAL FOR ALL MODELS) as common for all temperature based ET_o models considered in this study. Condition is set in the model to ignore LST values less than 0 ^{0}C and more than 46 ^{0}C

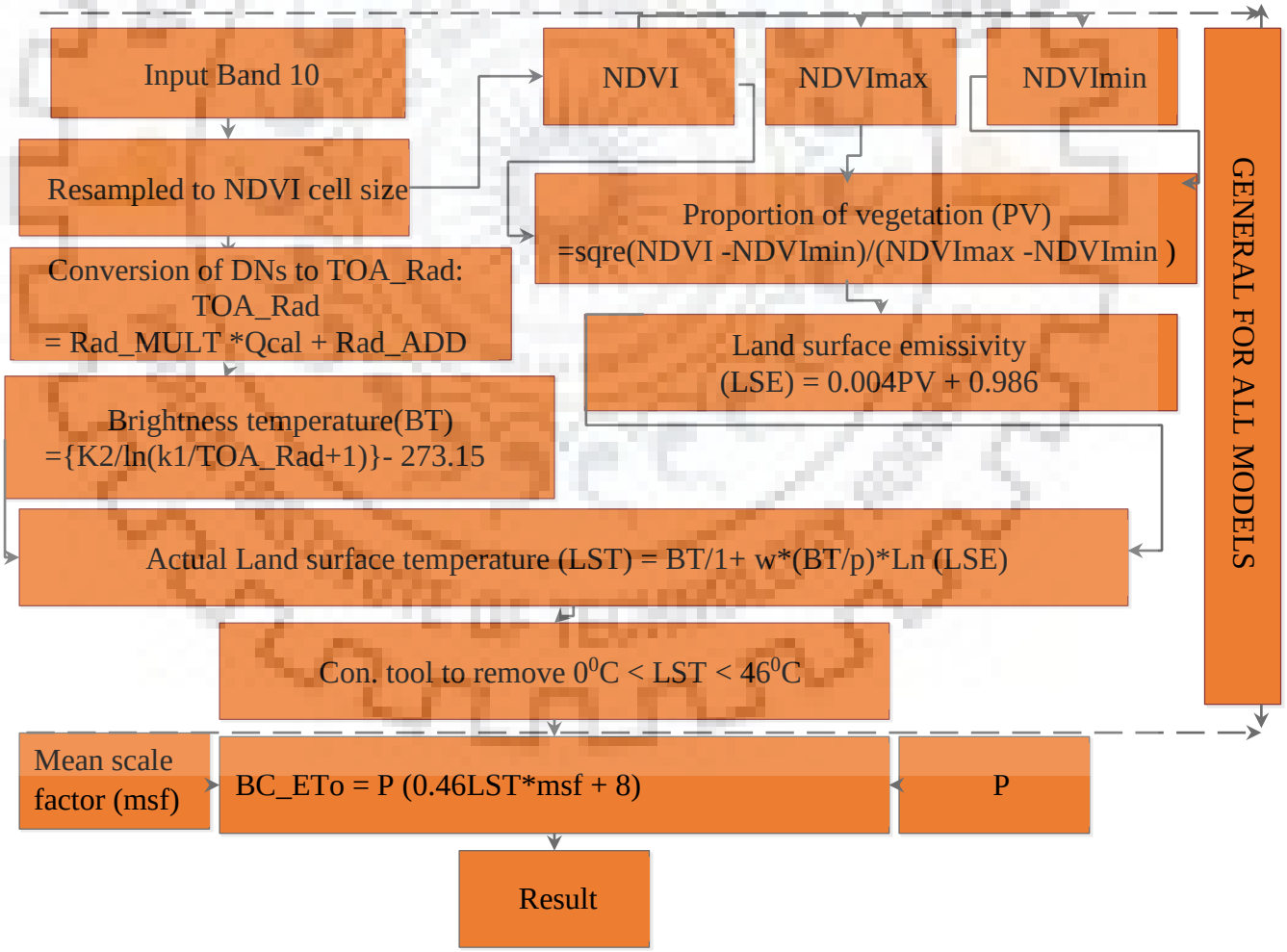

Figure 3. 5: Schematic framework for computation of ETo by Blaney-criddle model using Landsat 8 derived temperature based method

Top of Atmosphere Spectral Radiance (Lλ): Digital numbers (DNs) of Band 10 are converted into top of atmosphere spectral radiance using the formula obtained from USGS Website (https://landsat.usgs.gov/using-usgs-landsat-8-product) and given as below:

$L\lambda = M_L \times Q_{cal} + A_L$ ..... (8)

Where Lλ is radiance in w sr^{-1} m^{-2}, M_L is the band-specific multiplicative rescaling factor, Q_{cal} is the Band Digital numbers (DNs) i.e. raw image itself, A_L is the band-specific additive rescaling factor. M_L and A_L are provided in file metadata. However, in this document the following symbols are used instead of the above symbols; TOA_RAD for L_λ, Rad_MULT for M_L and Rad_ADD for A_L

The values of Rad_mult and Rad_ADD are 0.0003342 and 0.1 respectively. They are relatively constant for all images.

Conversion of radiance to brightness temperature: Once, DNs are converted to top of the atmospheric radiance, satellite or brightness temperature is computed from the TOA_RAD using the formula given below (https://landsat.usgs.gov/using-usgs-landsat-8-product)

$$BT = \left(\frac{K_2}{In\left(\frac{K1}{TOA-Rad}+1\right)}\right) - 273.15 \quad \text{..... (9)}$$

In which BT = brightness temperature in ^{0}C, k1 and K2 are band thermal constants available in metadata of the image's file. And 273.15 is the conversion factor from kelvins to degree Celsius. For band 10 of the chosen areas images, K1 is 774.8853 and K2 is 1321.0789.

Normalized Difference Vegetation index (NDVI) is computed by a separate model using the relation (Singh et al. 2010):

$$NDVI = \frac{NIR\ (band\ 5) - R\ (band\ 4)}{NIR\ (band\ 5) + R\ (band\ 4)} \quad \text{... ... ... (10)}$$

Where NIR is near infrared band (band 5) and R is Red band (band 4). Model is given below

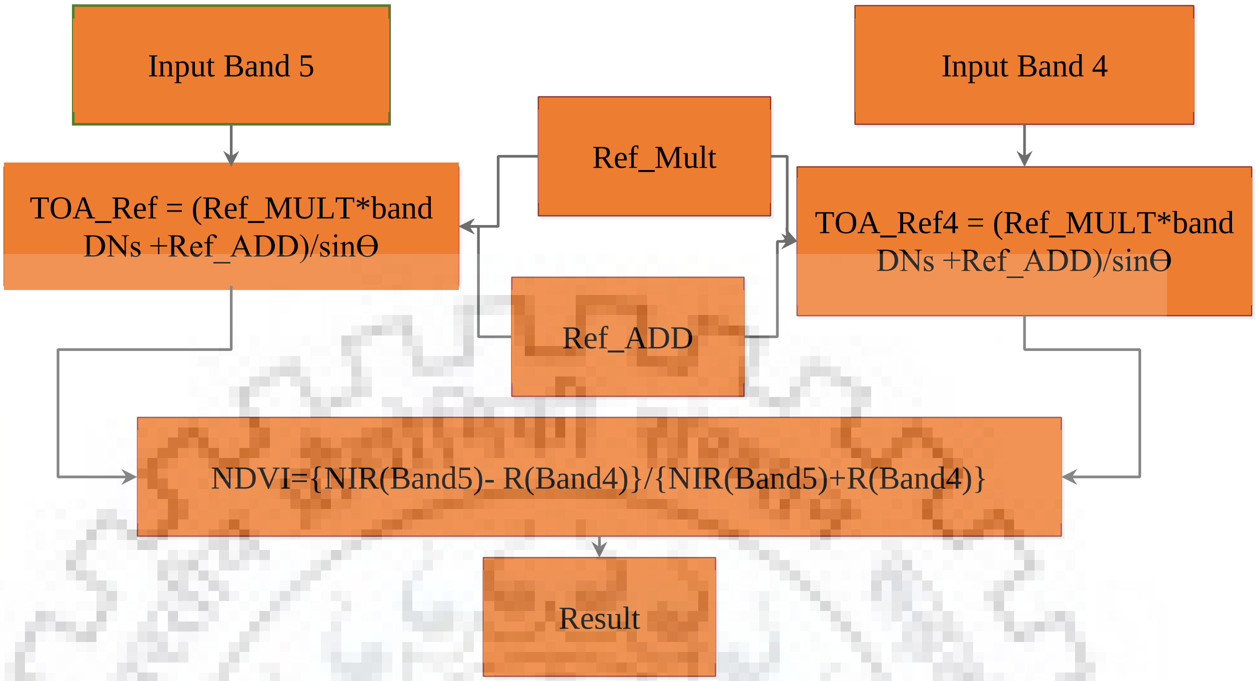

Figure 3. 6: Schematic framework used for computation of NDVI

For conversion of reflectance digital numbers (DNs) to top of atmosphere reflectance (TOA_Ref) and sun angle correction, the model use the following equation, given in USGS page (https://landsat.usgs.gov/using-usgs-landsat-8-product) to get top of atmosphere reflectance (TOA_Ref) prior to NDVI calculation:

TOA_Ref = (Ref_MULTxband DNs +Ref_ADD)/sin (Θ). …………………… (11)

Where Θ is sun elevation angle, Ref_MULT is band's reflectance multiplicative rescaling factor and Ref_ADD is band's reflectance additive rescaling factor, both given in metadata file. For the images of the chosen areas, Ref_mult is 0.00002 and Ref_ADD is -0.1. In calculation of NDVI, the parameter sin (Θ) in the above relation cancels out for two bands and doesn't need to be involved in computation.

The proportion of vegetation (PV) is calculated using a simple equation given by (Carlson & Ripley, 1997)

$$PV = \text{square}\left(\frac{\text{NDVI}-\text{NDVImin}}{\text{NDVImax}-\text{NDVImin}}\right) \ldots\ldots (12)$$

Where $NDVI_{max}$ and $NDVI_{min}$ are maximum and minimum NDVI values respectively.

Lands surface emissivity (LSE) : LSE is computed by using the equation proposed by (Giannini et al. 2015)

LSE = 0.004PV + 0.986 ……. (13)

Where, PV is proportion of vegetation

Land surface temperature with different land cover considered is calculated as: (Stathopoulou & Cartalis, 2007) and (Weng, Lu, & Schubring, 2004)

LST = BT/1+ wx(BT/p)xLn (LSE)……..…….(14)

Where LST is land surface temperature, w is band wavelength, P is constant = hc/σ (14380), h is Planck's constant (6.626*10^-34J*s), σ is Boltzmann constant (1.38*10^-23 J/K), and c is velocity of light (2.998*10^8 m/s) and other variables as defined previously.

Lastly, the model use the following relation to get ETo by Blaney-Criddle method (BC_ET_o), in mm/day (average monthly)

BC_ET_o = P (0.46LSTxmsf + 8) ……..….. (15)

Where LST is land surface temperature, msf is scaling factor obtained from NCEP data, P is percent of day light hours. P is function of latitude of a place and month of the year. Thus, Standard values of P are adopted from literature.

3.4.1.1.2 Thornthwaite ET_o model

The algorithm was created in ArcGIS 10.4 to compute ETo based on Thronthwaite method, from Landsat 8 imageries. The model inputs are month of interest LST (moi_LST) and land surface heat index (i) of different months in a season. The procedures used by algorithm are presented in figure 3.7

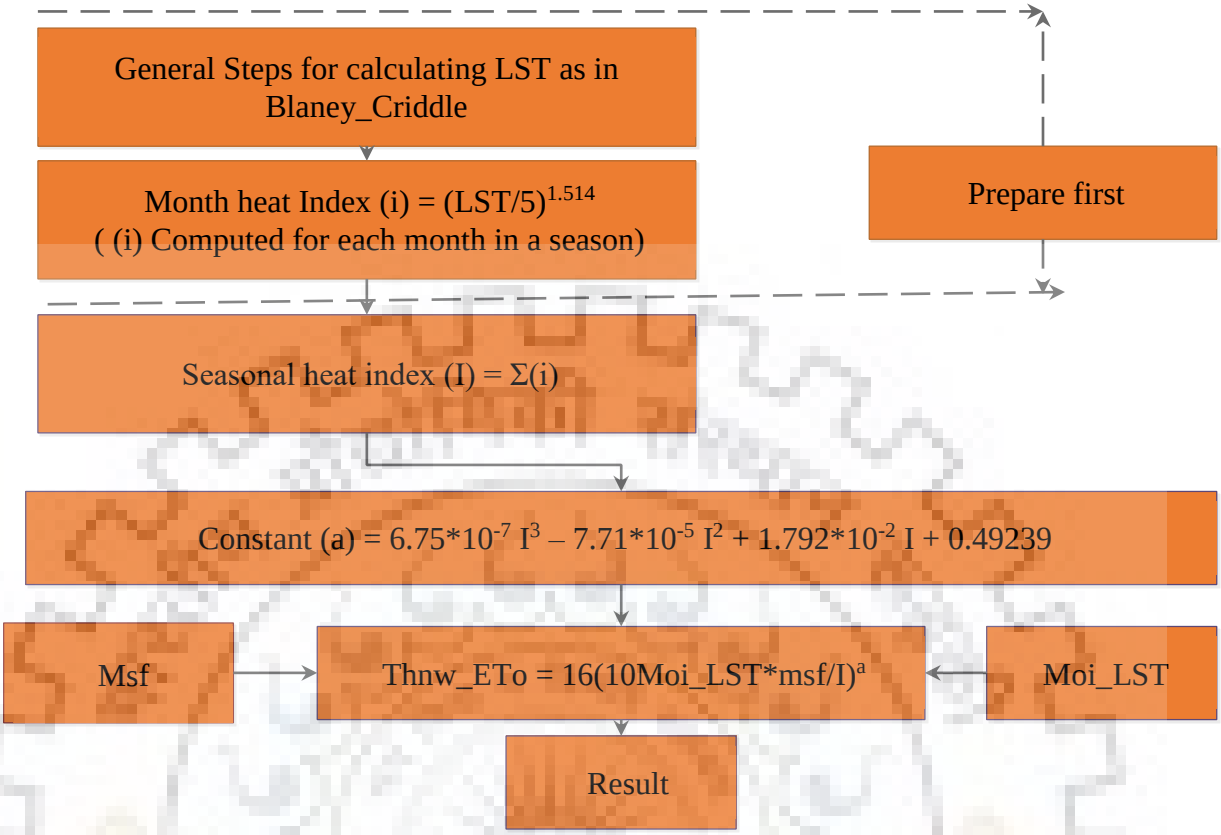

Figure 3. 7: Schematic framework for computation of ETo by Thornthwaite model using Landsat 8 derived temperature based method

3.4.1.1.3 Hargreaves (1985) ET_o model

The algorithm developed in ArcGIS 10.4, for computation of ETo by by Hargreaves original equation is given in figure 3.8. The model inputs are band 10, NDVI, $NDVI_{max}$, $NDVI_{min}$, extraterrestrial radiation value (Ra). Maximum, minimum and mean LST scaling factors are obtained as mentioned in the previous section. Ra is a function of latitude and period of year and it's obtained from standard values available in literature.

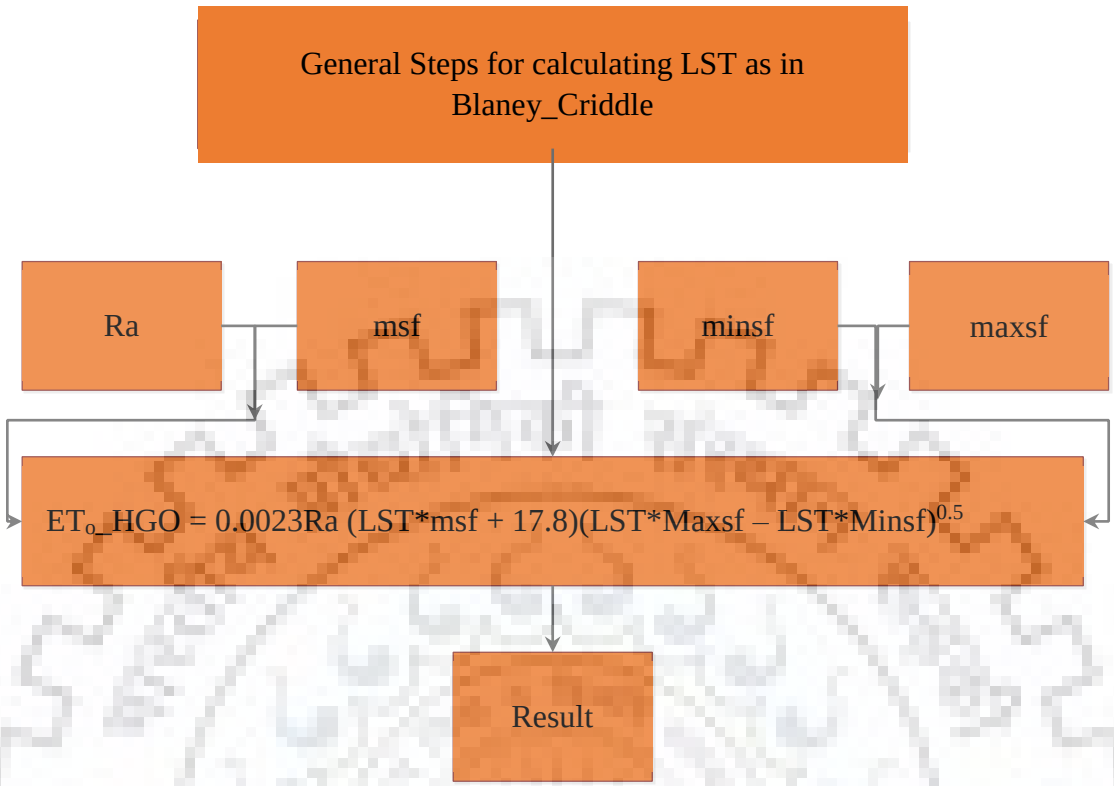

Figure 3. 8:Schematic framework for computation of ETo by Hargreaves model using Landsat 8 derived temperature based method

Note that in the flow chart, msf, minsf and maxsf refer to mean, minimum and maximum LST scaling factors respectively.

3.4.1.1.4 ET_o model for three modified versions of Hargreaves equation:

$ET_o = 0.408x0.0030xRa\ (Tmean + 20)(Tmax - Tmin)^{0.4}$ …….(16)

$ET_o = 0.408x0.0025xRa\ (Tmean + 16.8)(Tmax - Tmin)^{0.5}$ ……..(17)

$ET_o = 0.0023xRa\ (Tmean + 17.8)(Tmax - Tmin)^{0.424}$ ……...(18)

The algorithm for each of the three modified Hargreaves' equations above are similar to that of original Hargreaves equation presented above except in some numerical variables. So similar computational steps were followed by replacing the appropriate numerical values in each equation.

3.4.1.1.5 Kharrufa ET_o model

The inputs for kharrufa ETo algorithm are the same as in Blaney-Criddle model and is schematically represented as given figure 3.9 below:

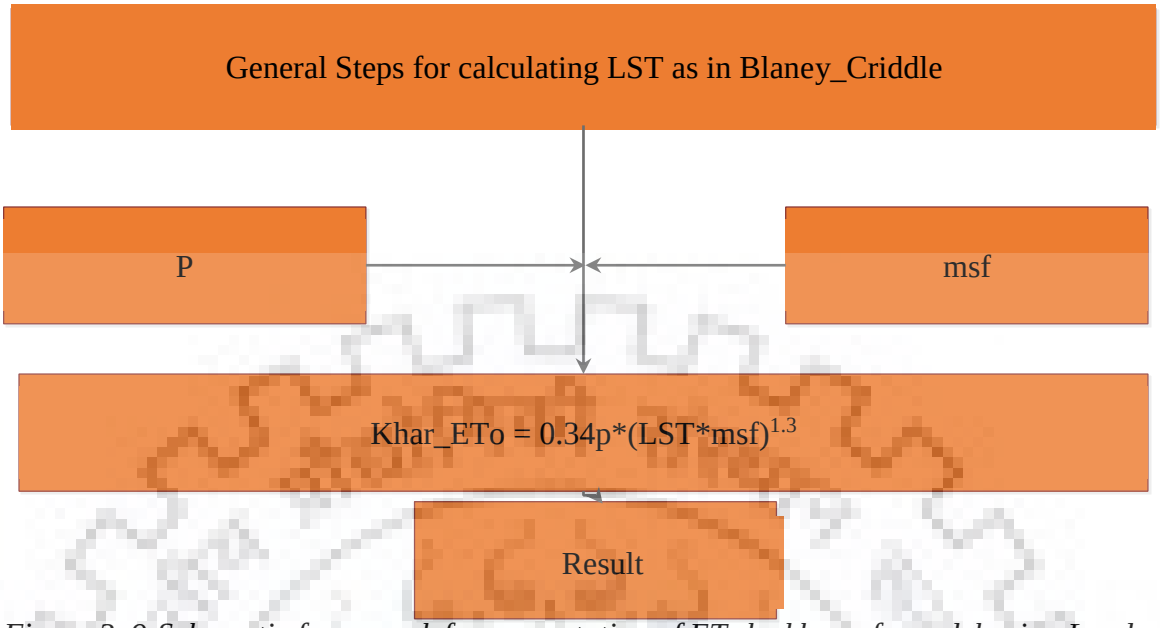

Figure 3. 9:Schematic framework for computation of ET_o by kharrufa model using Landsat 8 derived temperature based method

3.4.2 ASSESSMENT OF ET_O USING MODIS LST

8-day MODIS land surface temperature images (MOD11A2) were downloaded and were projected to geographic coordinate system (datum WGS84) in ENVI 5.3. Images with no data pixels were first converted to points and then interpolated using nearest neighborhood interpolation technique in ArcGIS spatial analyst tool. Further, 8 day LST products were aggregated into monthly scale and re-projected to UTM coordinate system (datum WGS84) and subsetted to the area of interest and for Roorkee which lies between two tiles, mosaicking is done prior to subsetting.

Rescaling was done using the factor 0.002, as per the metadata file of the LST images and converted to degree Celsius from Kelvin. LST extracted from the images acquired during day time and night time were considered as maximum and minimum respectively. The appropriate finished product(s) of the above processes were then used in computation of ET_o in the appropriate method.

A simple raster images processing model, was built in ArcGIS 10.4, for each of the ET_o methods to calculate the ET_o values from MODIS LST. The general schematic form of the stated model is presented in figure 3.10.

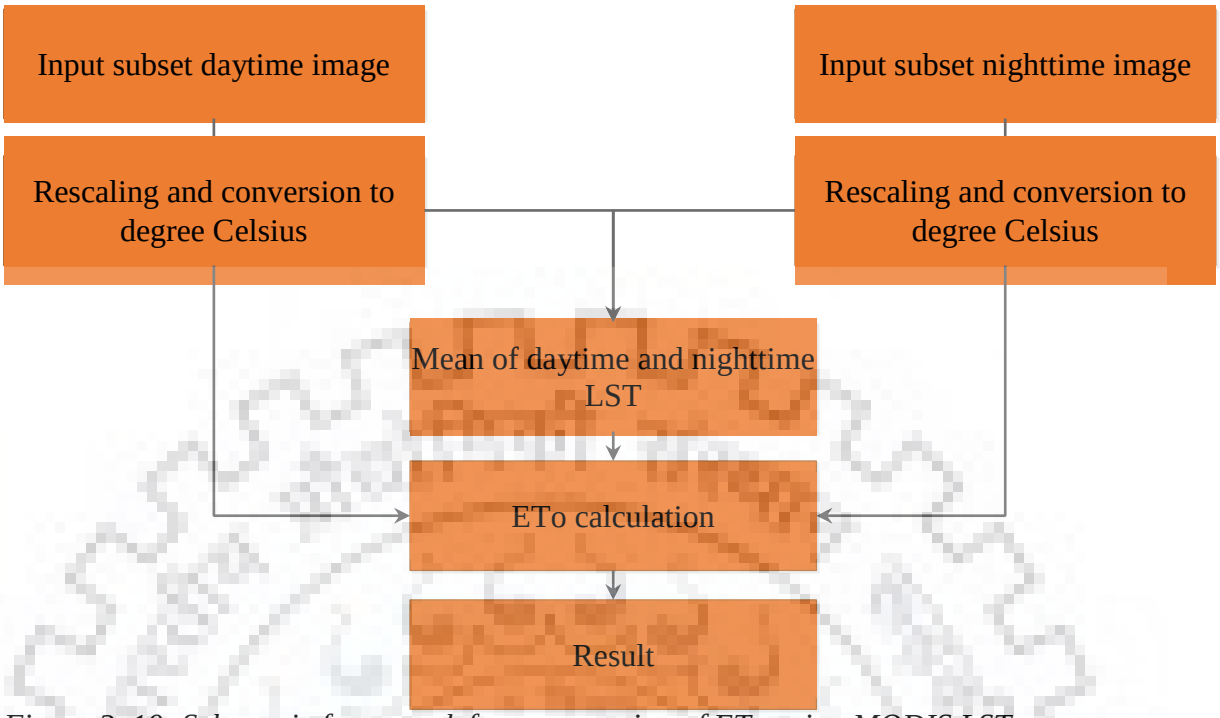

Figure 3. 10: Schematic framework for computation of ETo using MODIS LST

3.5 CALIBRATION AND EVALUATION CRITERIA

Several researchers recommended calibration for enhancing the performance of temperature based methods (Trajkovic, 2005; Fooladmand, Zandilak, & Ravanan, 2008). In this study, FAO Penman-Monteith method is used as reference model because it is recommended as best method (Allen et al., 1998) and has been used as standard in many researches (Issn & Estadual, 2016; Tabari & Grismer, 2013; Othoman et al. 2006; Pandey et al. 2016) etc. The equation is expressed as (Allen et al., 1998)

$$ETo = \frac{0.408\Delta(Rn-G)+\gamma\frac{900}{T+273}u2(es-ea)}{\Delta+\gamma(1+0.34u2)} \quad \text{.....(19)}$$

Where, ET_o is reference evapotranspiration in mm/day; R_n is net radiation in MJ/m^2/day; G is soil heat flux in MJ/m^2/day; T is mean daily air temperature in ^{0}C at reference height (2m); u_2 is wind speed in m/s at reference height; e_s-e_a is saturation vapour pressure deficit in kPa; e_s is saturation vapor pressure in kPa; e_a is the actual vapor pressure in kPa; Δ is slope of vapor pressure curve in kPa/^{0}C and γ is psychometric constant kPa/ °C.

3.5.1 Juba County station data

The monthly averages of temperature (maximum and minimum) was collected from Juba international airport station, located at altitude 457 m above mean sea level, latitude 4.86^{0}N and 31.6^{0}E . The data is given in table 3.5.

Table 3. 5: Juba station temperature data

Year	2013		2014		2015	
Month	Monthly Max. T, ^{0}C	Monthly Min T, ^{0}C	Monthly Max. T, ^{0}C	Monthly Min T, ^{0}C	Monthly Max. T, ^{0}C	Monthly Min T, ^{0}C
January	37.5	19.8	33.3	18.5	35.9	17.9
February	39.0	20.4	33.4	18.3	37.9	22.1
March	38.1	22.5	27.6	22.4	37.5	23.8
April	35.6	22.6	35.1	23.1	33.4	21.9
May	34.1	22.9	33.3	23.0	34.9	22.3
June	33.1	22.6	31.8	21.8	32.7	23.2
July	31.6	22.0	31.5	21.9	33.5	21.7
August	32.3	21.3	31.2	21.7	33.8	21.0
September	32.9	23.2	32.3	21.6	34.4	21.3
October	33.0	22.9	32.3	21.9	33.5	20.3
November	33.6	22.0	34.3	21.6	33.4	21.0
December	35.7	20.6	35.8	20.3	34.7	20.2

3.5.2 Roorkee region data

The daily 1^0x1^0 IMD gridded temperature data (maximum and minimum) was aggregated to monthly and then used in Cropwat software for evaluation of modelling methods as cited in the previous section. However, prior to application, the aggregated monthly maximum and minimum temperature at four gridded stations {(29.5^0N/77.5^0E), (29.5^0N/78.5^0E), (30.5^0N/77.5^0E), (30.5^0/78.5^0E)} that surrounded Roorkee region were first interpolated in ArcGIS 10.4 using Inverse Distance Weighted (IDW) interpolation technique. This was done because there is no single gridded station in the selected region of Roorkee and so after interpolation, the single point (29.85^0N/77.88^0E) values were used in Cropwat.

3.5.3 Estimation of missing data for FAO Penman-Montieth method application

ET_o was computed using cropwat 8.0 software, as this particular software has capability to estimate ET_o with limited weather data. The software has an option of computing reference crop evapotranspiration using maximum and minimum temperatures, based on FAO Penman-Montieth method. Methodology for estimation of parameters required for estimation of ET_o is adopted from FAO irrigation and drainage paper -56 (Allen et al., 1998). It is indicated that error produce by FAO-

PM method based on temperature are low for monthly or higher periods (Hess & White, 2009) and so is adopted in this study as standard because ET_o estimation is for longer period; monthly.

Further, ET_o estimated using remote sensing techniques for any identified pixel is calibrated with reference to the meteorological data corresponding to same meteorological station using simple linear regression analysis.

$$ET_o\_cal = a + bET_o\_sat \quad \text{(20)}$$

Where ET_o_cal represent the calibrated ET_o and ET_o_sat is ET_o estimated from satellite data. "a" and "b" are obtained by regression analysis between Penman-Montieth equation as standard with ETo_sat.

Coefficient **a** and **b** can be estimated by the following equations of least squares method.

$$b = \Sigma (ET_{o\_sat\_i} - ET_{o\_sat\_avg})(ET_{o\_PM} - ET_{o\_PM\_ag}) / \Sigma (ET_{o\_sat\_i} - ET_{o\_sat\_avg})^2 \quad \text{(21)}$$

$$a = ET_{o\_PM\_avg} - b * ET_{o\_sat\_avg} \quad \text{(22)}$$

Comparison of models was done using standard statistics and linear regression analysis (Douglas et al. 2009)(Maeda et al., 2011). Root Mean Squared Error (RMSE), Mean Absolute Error (MAE), Percentage Error (PE) and coefficient of determination (R^2) were computed using the equations described below:

$$RMSE = (1/n\Sigma (ET_o\_cal - ET_0\_PM)^2)^{0.5} \quad \text{(23)}$$

$$MAE = 1/n\Sigma \left| ET_o\_cal - ET_o\_PM \right| \quad \text{(24)}$$

$$PE = (ET_o\_cal - ET_o\_PM)/ET_o\_PM * 100 \quad \text{(25)}$$

$$R^2 = SSR/SST = 1 - SSE/SST \quad \text{(26)}$$

Where SSR, SST and SSE are sum of squares due to regression, sum of squares for the total deviation and sum of squares for the error respectively and are calculated as follows.

$$SSR = \Sigma (ETo\_cal - ETo\_cal\_avg)^2 \quad \text{(27)}$$

$$SST = \Sigma (ETo\_PM - ETo\_PM\_avg)^2 \quad \text{(28)}$$

$$SSE = \Sigma (ETo\_PM - ETo\_cal)^2 \quad \text{(29)}$$

SST = SSR +SSE …….……. (30)

CHAPTER IV

RESULTS AND DISCUSSIONS

In this chapter, results obtained from this study and their comparison with FAO Penman-Montieth are presented and analyzed.

4.1 LOCATION 1 (JUBA COUNTY, SOUTH SUDAN)

4.1.1 RESULTS

The results for analysis were obtain from a pixel value at same latitude and longitude as Juba weather station. The monthly results obtained in the dry season of 2014-2015 (i.e. November 2014 to February 2015), before models' calibration are presented together with FAO-PM values in table 4.1 and their deviations (errors) from standard FAO-PM values, in percent and in mm/day are shown in Tables 4.2 and 4.3 respectively. It can be seen that KHARRUFA MODIS based, ALLEN (1993) and DROOGERS et al. (2002) modified Hargreaves models deviate tremendously from FAO-PM values (Tables: 4.2 and 4.3). The KHARRUFA MODIS based method exhibited overestimation of the ETo values from 34% (1.96 mm/day) to 54% (2.7 mm/day) as presented in Tables 4.2 and 4.3. However, ALLEN (1993) and DROOGERS et al. (2002) modified Hargreaves method showed underestimation of the ETo values from 49% (2.41 mm/day) to 59% (3.42 mm/day) as also presented in Tables 4.2 and 4.3. Other models errors, before calibration ranges from 1 to 25% and can further be emphasized that among all the models, before calibration, Hargreaves (1985) Landsat based, performed better with deviation errors below 5% (i.e. < 0.3mm/day). The error and regression analysis results are presented in Table 4.4. Further, regression lines are presented in figure 4.1. It is observed from figure 4.1 that, models parameterized with Landsat 8 LST shown a best fit than models parameterized with MODIS LST and their R^2 ranges from 0.91 to 0.93, with Hargreaves (1985) model having the highest R^2 value (0.93).

RMSE and MAE were used to quantify the variations between ET_o estimates using standard method (FAO-PM) and the estimates obtained by empirical models based on remotely sensed LST. For Landsat 8 LST data, the seasonal RMSE and MAE of models were low, they ranged from 0.1064 to 0.1165mm/day and 0.0163 to 0.0997 mm/day respectively. Further, the Hargreaves (1985) Landsat-based models have lowest RMSE and MAE value, 0.1064 and 0.0163 mm/day respectively. And for MODIS LST data, RMSE and MAE of the models varied from 0.2591 to 0.3082mm/day and 0.132 to 0.264mm/day respectively. The results of the calibrated satellite based ET_o models are presented in table 4.5 and their variations from the standard are presented in Tables 4.6 and figure 4.7 .Further,

it is seen that all the errors, for all models are minimal when calibrated, tables (4.6 & 4.7). Further, satellite and ground station data of three months, of Juba County, of different dry season (December 2013 to February 2014; months whose Landsat 8 images were less contaminated by clouds, in this specific dry season) was used for validation and results are shown in table 4.8. The monthly deviations of validated satellite based ET_o models, from reference model are presented in tables 4.9 and 4.10. It is also observed in tables 4.9 and 4.10 that, ET_o models based on Landsat LST have low percentage errors (0 to 13%) except Thornthwaite (17%) in the month of December. While MODIS LST based ET_o models showed errors higher than Landsat ET_o models. MODIS models errors range from 5 up to 57% with Trajkovic (2007) modified Hargreaves showing low errors (5 to 18%) and Thornthwaite showing highest errors (43 to 57%). In Juba County, Hargreaves model based on Landsat 8 data appears best during the study period, with overall RMSE of 0.1064 mm/day, MAE of 0.0163mm/day, R^2 of 0.93 and produces reasonable monthly errors as observed in tables (4.2, 4.3, 4.6, 4.7, 4.9 & 4.10. Thus, Hargreaves-Landsat 8 based model was used to prepare ET_o maps of three months (showing average of two dry seasons of 2013-2013 and 2014-2015). The ET_o maps are presented in figures 4.2, 4.3 and 4.4 for December, January and February respectively.

4.1.2 DISCUSSION

In Juba County, South Sudan, the results showed that, before calibration, the departure of LST ET_o models values from FAO-PM method values was very high. Only Hargreaves (Landsat) model produced error less than 5% and thus, calibration was done, using FAO-PM method as standard with ground station data, to reduce the departure of simulated ET_o values from reference values.

After calibration, it was found that, Landsat ET_o models showed close relationship with FAO-PM values than MODIS ET_o methods (table 4.2). This may be due to different spatial resolution of the MODIS and Landsat satellite data. Because coarse spatial resolution of MODIS data does not consider land surface heterogeneity and this was also corroborated from the previous studies. (Li et al., 2017; Kustas et al. 2003). Xiaozhou et al. (2005).observed that, MODIS data cause major errors in estimating any of the land surface energy fluxes like evapotranspiration.

However, to assure the relative confident in the prediction of ET_o using satellite derived LST, the calibrated satellite LST ET_o models were validated by predicting other season's ET_o values. Hargreaves (1985) ET_o model, based on Landsat, shown good results with high R^2 value (0.93) and less RMSE (0.1064mm/day) and less MAE (0.0163mm/day) (table 4.4) and it is worth mentioning

that, this performance (of Landsat Hargreaves ET_o), against standard FAO Penman Montieth, is relatively the same or better than the performance of air temperature based Hargreaves's found in some studies, in other places. For example, one study carried out in Iran by Hosseinzadeh Talaee, (2014) found R^2 of 0.89, RMSE of 1.447mm/day and MAE of 1.246, and this performance of Hargreaves parameterized with air temperature, is little lower than in the current study. Similarly in other study done in Sebia (Trajkovic, 2005), in which the Hargreaves (1985) model was evaluated against FAO PM method, obtained RMSE of 0.371mm/day and MAE 0.306mm/day and this performance is almost in the same error bracket with the finding in the present study, in which RMSE was 0.1064mm/day and MAE of 0.0163mm/day. Also in other study conducted in Kenya, East Africa (Maeda et al., 2011) in which Hargreaves (1985) ET_o model was parameterized with MODIS LST and evaluated against FAO PM method, found correlation coefficient (R) of 0.67, RMSE of 0.47mm/day and MAE of 0.39mm/day , while Hargreaves (1985) Landsat ET_o model proposed in this study, have better performance than that. The correlation coefficient, RMSE and MAE of were 0.96, 0.1064mm/day and 0.0163mm/day respectively, for Hargreaves (1985) Landsat ET_o model.

Thus, it can be stated that, the proposed Hargreaves (1985) Landsat based ET_o model can be employed in the study area for ET_o computation, provided that the Landsat images are not contaminated by clouds. To help in irrigation planning, the ET_o maps of Juba County, showing average spatial variation of ET_o, for three months, in dry season, were prepared as presented in figures 4.2, 4.3 & 4.4, for December, January and February respectively. And it can be seen from the ET_o maps prepared by Landsat 8 Hargreaves, ET_o model, showing average of ET_o values of three months in two dry seasons that ET_o have its highest in February (figure 4.4), and this may be due to increase in both LST and air temperature in February as presented in chapter III; table 3.3. Thus, the selected satellite model can be used for ET_o estimation in the study area when no ground station data input for conventional ET_o models is available and has a benefit of obtaining ET_o values for heterogeneous area spatially.

Table 4. 1: Satellite ET_o Models Results before calibration (2014-2015), mm/day; Juba County

Month/Model	November	December	January	February
FAO-PM ETo	4.97	5.45	5.77	6.03
HargO_ L8. ETo	4.83	5.4	5.52	6.17
HargO_ Md ETo	5.91	5.63	6.00	6.33
HargT_L8. ETo	3.97	4.40	4.49	5.00
HargT_ Md ETo	4.84	4.63	4.89	5.18
HargA_ L8. ETo	2.10	2.31	2.35	2.61
HargA_Md ETo	2.52	2.42	2.55	2.70
HargD_ L8. ETo	2.10	2.34	2.39	2.68
HargD_Md ETo	2.56	2.45	2.61	2.75
Khar_ L8. ETo	5.32	6.33	6.38	6.82
Khar_Md ETo	7.67	7.86	7.73	8.16
BC. L8. ETo	5.10	5.51	5.53	5.70
BC. Md_ETo	5.90	5.97	5.92	6.07
Thw L8 ETo	3.72	4.40	4.43	4.72
Thw Md ETo	5.44	5.60	6.02	5.75

Table 4. 2: Monthly percentage deviation (error) of different satellite models from FAO-PM before calibraton (Season 2014/2015); Juba County

Month/ETo model	Deviation of different satellite LST ETo model before calibration (%)			
	November	December	January	February
HargO_ L8. er	-3%	-1%	-4%	2%
HarggO_ Md er	19%	3%	4%	5%
HargT_L8. er	-20%	-19%	-22%	-17%
HargT_ Md er	-3%	-15%	-15%	-14%
HargA_ L8. er	-58%	-58%	-59%	-57%
HargA_Md er	-49%	-56%	-56%	-55%
HargD_ L8. er	-58%	-57%	-59%	-56%
HargD_Md er	-48%	-55%	-55%	-54%
Khar_ L8. er	7%	16%	11%	13%
Khar_Md er	54%	44%	34%	35%
BC. L8. er	3%	1%	-4%	-5%
BC. Md_er	19%	10%	3%	1%
Thw L8 er	-25%	-19%	-23%	-22%
Thw Md er	9%	3%	4%	-5%

Table 4. 3: Monthly deviation (error) of different models from FAO-PM before calibration, in mm/day (Season 2014/2015); Juba County

Month/ETo model	Deviation of different satellite LST ETo model before calibration, in mm/day			
	November	December	January	February
HargO_ L8. er	-0.14	-0.05	-0.25	0.14
HargO_ Md er	0.94	0.18	0.23	0.30
HargT_L8. er	-1.00	-1.05	-1.28	-1.03
HargT_ Md er	-0.13	-0.82	-0.88	-0.85
HargA_ L8. er	-2.87	-3.14	-3.42	-3.42
HargA_Md er	-2.45	-3.03	-3.22	-3.33
HargD_ L8. er	-2.87	-3.11	-3.38	-3.35
HargD_Md er	-2.41	-3.00	-3.16	-3.28
Khar_ L8. er	0.35	0.88	0.61	0.79
Khar_Md er	2.70	2.41	1.96	2.13
BC. L8. er	0.13	0.06	-0.24	-0.33
BC. Md_er	0.93	0.52	0.15	0.04
Thw L8 er	-1.25	-1.05	-1.34	-1.31
Thw Md er	0.47	0.15	0.25	-0.28

Table 4. 4: Summary of regression and overall error analysis (2014-2015); Juba County

Model	Satellite data used	R^2	R	RSME mm/day	MAE Mm/day	Developed regression equations Y= dependent variable X= ET_o estimated from satellite data
BC	Landsat 8	0.92	0.96	0.1123	0.0954	Y = 1.7184X - 3.8274
	MODIS	0.56	0.75	0.2627	0.2102	Y = 4.4913X - 21.236
HargO	Landsat 8	0.93	0.96	0.1064	0.0163	Y = 0.7997X + 1.1727
	MODIS	0.39	0.63	0.3075	0.132	Y = 0.9943X - 0.3784
HargT	Landsat 8	0.92	0.96	0.1103	0.0944	Y = 1.0369X + 0.9251
	MODIS	0.39	0.63	0.3082	0.264	Y = 1.2609X - 0.6043
HargD	Landsat 8	0.92	0.96	0.1122	0.096	Y = 1.8383X +1.1844
	MODIS	0.44	0.66	0.3000	0.2532	Y = 2.4217X - 0.7233
HargA	Landsat 8	0.91	0.96	0.1165	0.0997	Y = 2.0837X + 0.6740
	MODIS	0.42	0.65	0.3019	0.2575	Y = 2.5438X - 0.9252
Kharr	Landsat 8	0.92	0.96	0.1102	0.0931	Y = 0.6910X + 1.2622
	MODIS	0.57	0.76	0.2591	0.2061	Y = 1.5794X - 6.8514
Thw	Landsat 8	0.92	0.96	0.1117	0.0944	Y = 1.0357X + 1.0836
	MODIS	0.57	0.76	0.2689	0.2237	Y = 1.4107X - 2.4869

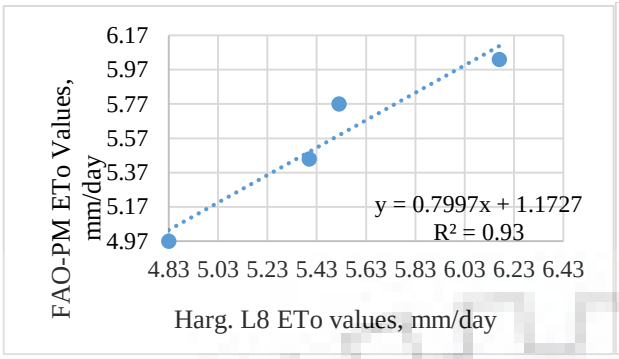
FAO-PM ETo Values, mm/day
6.17
5.97
5.77
5.57
5.37
5.17
4.97
4.83 5.03 5.23 5.43 5.63 5.83 6.03 6.23 6.43
y = 0.7997x + 1.1727
R² = 0.93
Harg. L8 ETo values, mm/day

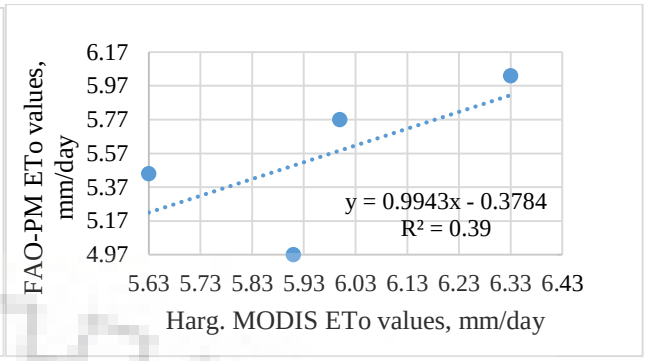
FAO-PM ETo values, mm/day
6.17
5.97
5.77
5.57
5.37
5.17
4.97
5.63 5.73 5.83 5.93 6.03 6.13 6.23 6.33 6.43
y = 0.9943x - 0.3784
R² = 0.39
Harg. MODIS ETo values, mm/day

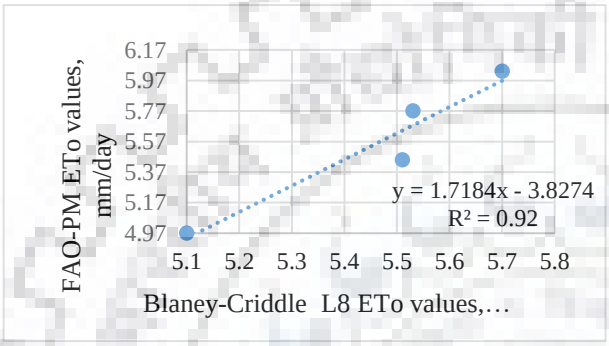
FAO-PM ETo values, mm/day
6.17
5.97
5.77
5.57
5.37
5.17
4.97
5.1 5.2 5.3 5.4 5.5 5.6 5.7 5.8
y = 1.7184x - 3.8274
R² = 0.92
Blaney-Criddle L8 ETo values,…

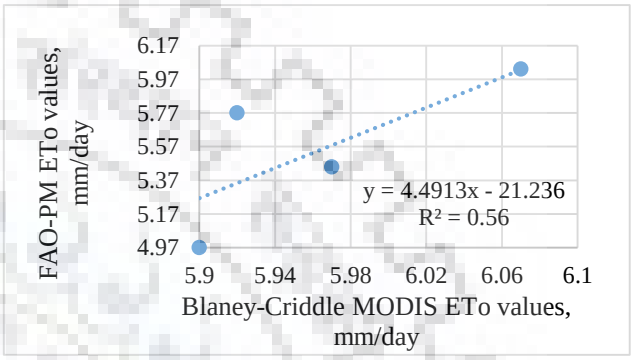
FAO-PM ETo values, mm/day
6.17
5.97
5.77
5.57
5.37
5.17
4.97
5.9 5.94 5.98 6.02 6.06 6.1
y = 4.4913x - 21.236
R² = 0.56
Blaney-Criddle MODIS ETo values, mm/day

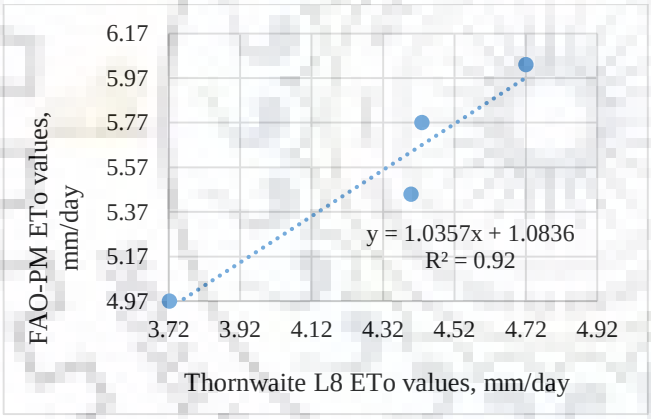
FAO-PM ETo values, mm/day
6.17
5.97
5.77
5.57
5.37
5.17
4.97
3.72 3.92 4.12 4.32 4.52 4.72 4.92
y = 1.0357x + 1.0836
R² = 0.92
Thornwaite L8 ETo values, mm/day

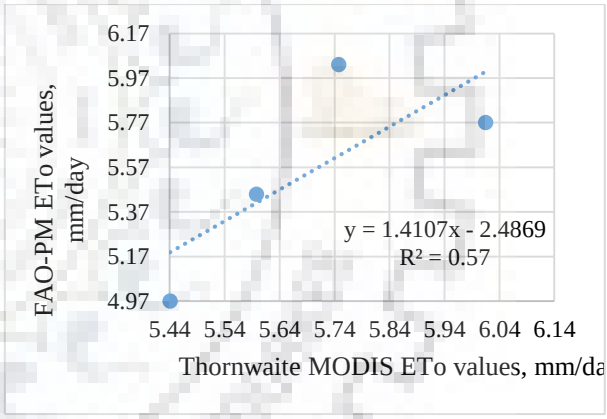
FAO-PM ETo values, mm/day
6.17
5.97
5.77
5.57
5.37
5.17
4.97
5.44 5.54 5.64 5.74 5.84 5.94 6.04 6.14
y = 1.4107x - 2.4869
R² = 0.57
Thornwaite MODIS ETo values, mm/da

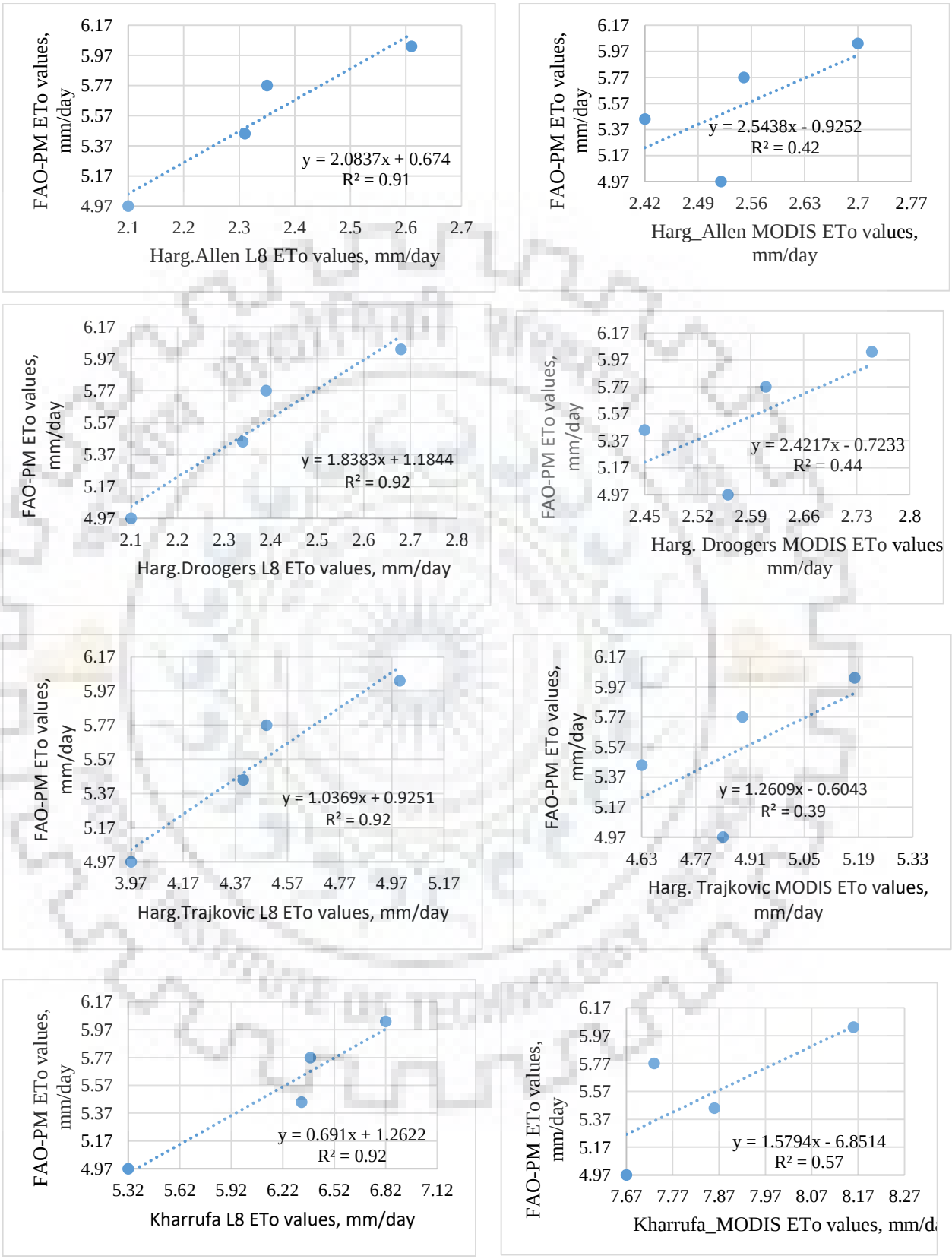

Figure 4. 1: Regression graphs of different satellite data - Juba County

Table 4. 5: ET_o Models Results after calibration (2014-2015), in mm/day; Juba County

Month/Model	November	December	January	February
FAO-PM ET_o	4.97	5.45	5.77	6.03
HargO_L8_ET_o	5.04	5.49	5.59	6.11
HargO_Md_ET_o	5.50	5.22	5.59	5.92
HargT_L8 ET_o	5.04	5.49	5.58	6.11
HargT_Md_ET_o	5.50	5.23	5.56	5.93
HargD_L8.ET_o	5.04	5.49	5.58	6.11
HargD_Md._ET_o	5.48	5.21	5.60	5.94
HargA_L8.ET_o	5.05	5.49	5.57	6.11
HargA_Md.ET_o	5.49	5.23	5.56	5.94
Kharr_L8.ET_o	4.94	5.64	5.67	5.97
Kharr_Md.ET_o	5.26	5.56	5.36	6.04
BC_L8_ET_o	4.94	5.64	5.68	5.97
BC_Md_ET_o	5.26	5.58	5.35	6.03
Thw_L8_ET_o	4.94	5.64	5.67	5.97
Thw_Md_ET_o	5.19	5.41	6.00	5.62

Table 4. 6: Monthly ET_o deviation (error) of different satellite Models from FAO-PM after calibration, in mm/day (season 2014/2015); Juba County

Month/ET_o model	Deviation of different satellite LST ET_o model, in mm/day			
	November	December	January	February
HargO_L8 er	0.07	0.04	-0.18	0.08
HargO_Md er	0.53	-0.23	-0.18	-0.11
HargT_L8 er	0.07	0.04	-0.19	0.08
HargT_Md er	0.53	-0.22	-0.21	-0.10
HargD_L8 er	0.07	0.04	-0.19	0.08
HargD_Md er	0.51	-0.24	-0.17	-0.09
HargA_L8 er	0.08	0.04	-0.20	0.08
HargA_Md er	0.52	-0.22	-0.21	-0.09
Kharr_L8 er	-0.03	0.19	-0.10	-0.06
Karr_Md er	0.29	0.11	-0.41	0.01
BC_L8 er	-0.03	0.19	-0.09	-0.06
BC_Md er	0.29	0.13	-0.42	0.00
Thw_L8 er	-0.03	0.19	-0.10	-0.06
Thw_Md er	0.22	-0.04	0.23	-0.41

Table 4. 7:Monthly percent errors of different satellite Models after calibration, in % (season 2014/2015); Juba County

Month/ETo model	Deviation of different satellite LST ET_o model, in percent.			
	November	December	January	February
HargO_L8 er	1%	1%	-3%	1%
HargO_Md er	11%	-4%	-3%	-2%
HargT_L8 er	1%	1%	-3%	1%
HargT_Md er	11%	-4%	-4%	-2%
HargD_L8 er	2%	1%	-3%	1%
HargD_Md er	10%	-4%	-3%	-2%
HargA_L8 er	2%	1%	-3%	1%
HargA_Md er	10%	-4%	-4%	-1%
Kharr_L8 er	-1%	3%	-2%	-1%
Karr_Md er	6%	2%	-7%	0%
BC_L8 er	-1%	4%	-2%	-1%
BC_Md er	6%	2%	-7%	0%
Thw_L8 er	-1%	3%	-2%	-1%
Thw_Md er	4%	-1%	4%	-7%

Table 4. 8**:** Satellite ET_o Models validation Results (dry season of 2013-2014), mm/day; Juba County

Month/Model	**Dec.**	**Jan**	**Feb**
FAO-PM	5.33	5.14	5.41
HargO_L8 ET_o	5.36	5.51	6.13
HargO_Md ET_o	5.63	5.98	6.46
HargT_L8 ET_o	5.35	5.51	6.14
HargT_Md ET_o	5.60	5.95	6.40
HargA_L8 ET_o	5.34	5.50	6.14
HargA_Md ET_o	5.60	5.95	6.42
HargD_L8 ET_o	5.35	5.51	6.13
HargD_Md ET_o	5.64	6.02	6.52
Khar_L8 ET_o	5.47	5.58	6.00
Khar.Md ET_o	5.74	6.38	5.87
BC_L8 ET_o	5.42	5.53	5.94
Bc_Md ET_o	5.75	6.42	5.88
Thw_L8 ET_o	4.42	4.52	4.96
Thw_Md ET_o	7.67	8.05	7.74

Table 4. 9: Monthly ET_o deviations of validation of different satellite ET_o Models in mm/day (dry Season of 2013/2014); Juba County

Month/ETo model	Deviation of different satellite LST ETo model, in mm/day		
	December	January	February
HargO_L8 er	0.03	0.37	0.72
HargO_Md er	0.30	0.84	1.05
HargT_L8 er	0.02	0.37	0.73
HargT_Md er	0.27	0.81	0.99
HargA_L8 er	0.01	0.36	0.73
HargA_Md er	0.27	0.81	1.01
HargD_L8 er	0.02	0.37	0.72
HargD_Md er	0.31	0.88	1.11
Khar_L8 er	0.14	0.44	0.59
Khar.Md er	0.41	1.24	0.46
BC_L8 er	0.09	0.39	0.53
Bc_Md er	0.42	1.28	0.47
Thw_L8 er	-0.91	-0.62	-0.45
Thw_Md er	2.34	2.91	2.33

Table 4. 10: Monthly ETo percent errors of different Models on validation (Season 2013/2014); Juba County

Month/ETo model	Deviation of different satellite LST ETo model, in percent.		
	December	January	February
HargO_L8 er	1%	7%	13%
HargO_Md er	6%	16%	19%
HargT_L8 er	0%	7%	13%
HargT_Md er	5%	16%	18%
HargA_L8 er	0%	7%	13%
HargA_Md er	5%	16%	19%
HargD_L8 er	0%	7%	13%
HargD_Md er	6%	17%	21%
Khar_L8 er	3%	9%	11%
Khar.Md er	8%	24%	9%
BC_L8 er	2%	8%	10%
Bc_Md er	8%	25%	9%
Thw_L8 er	-17%	-12%	-8%
Thw_Md er	44%	57%	43%

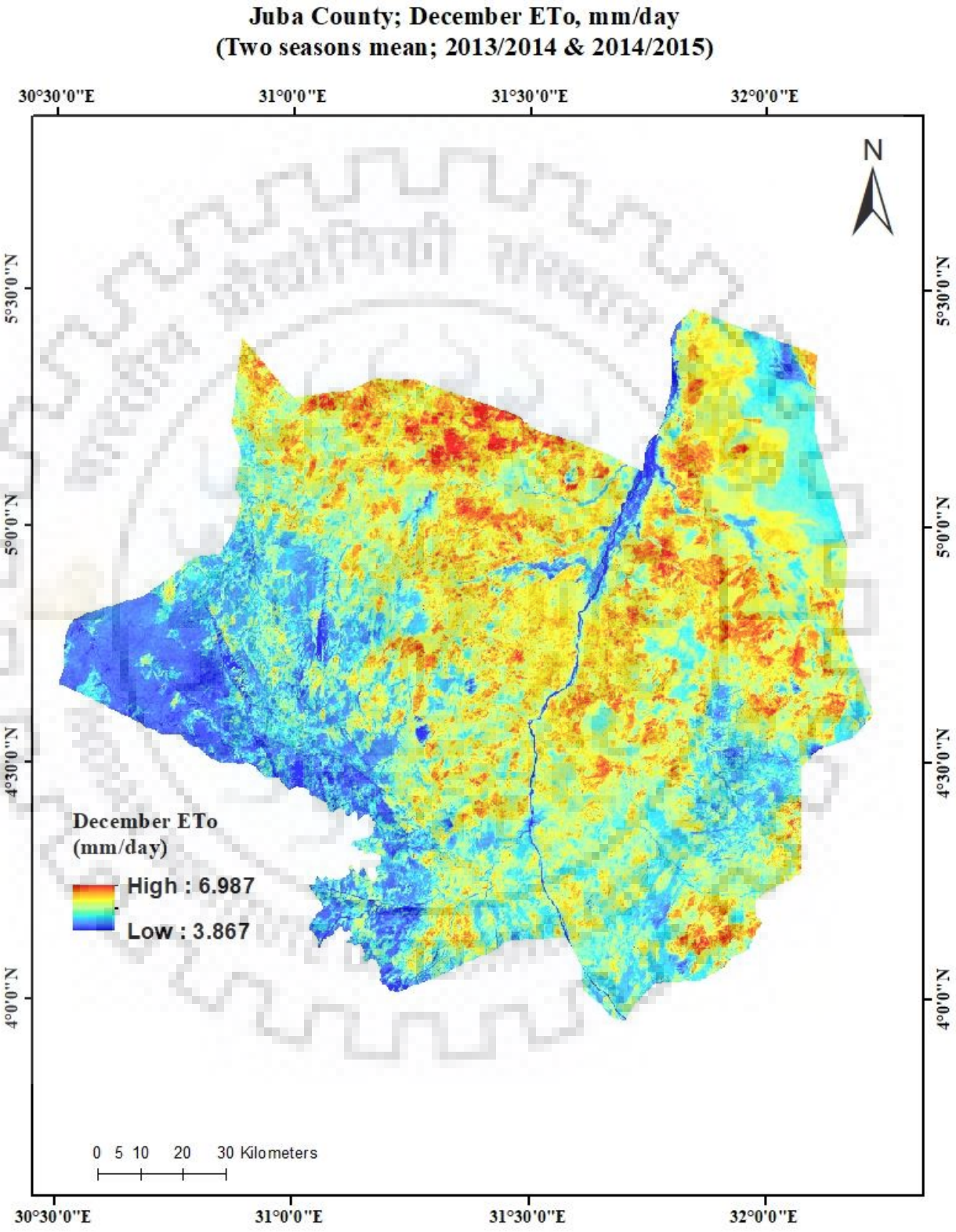

Figure 4. 2: ET_o map of Juba County for the month of December

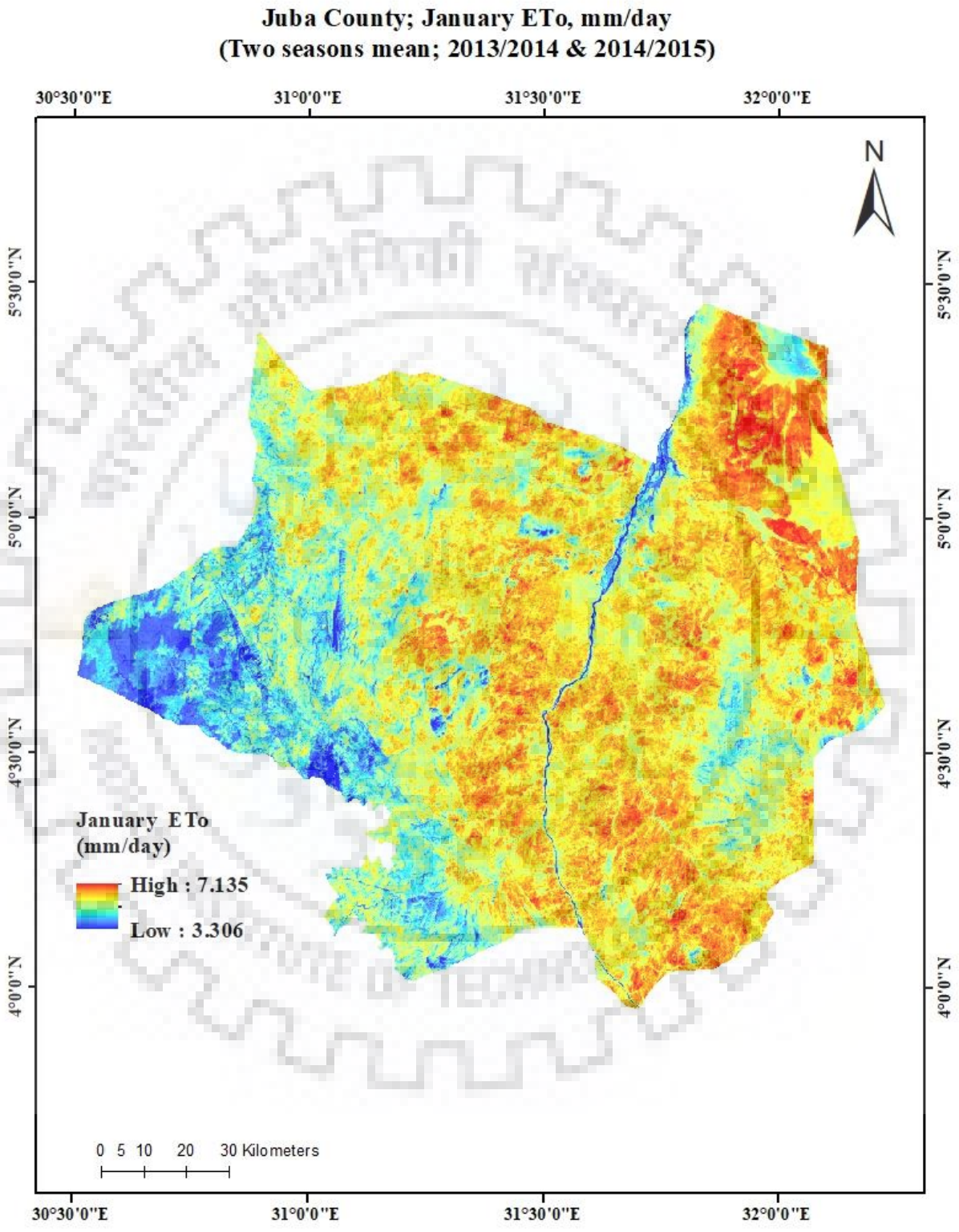

Figure 4. 3: ET_o map of Juba County for the month of Januaɪy

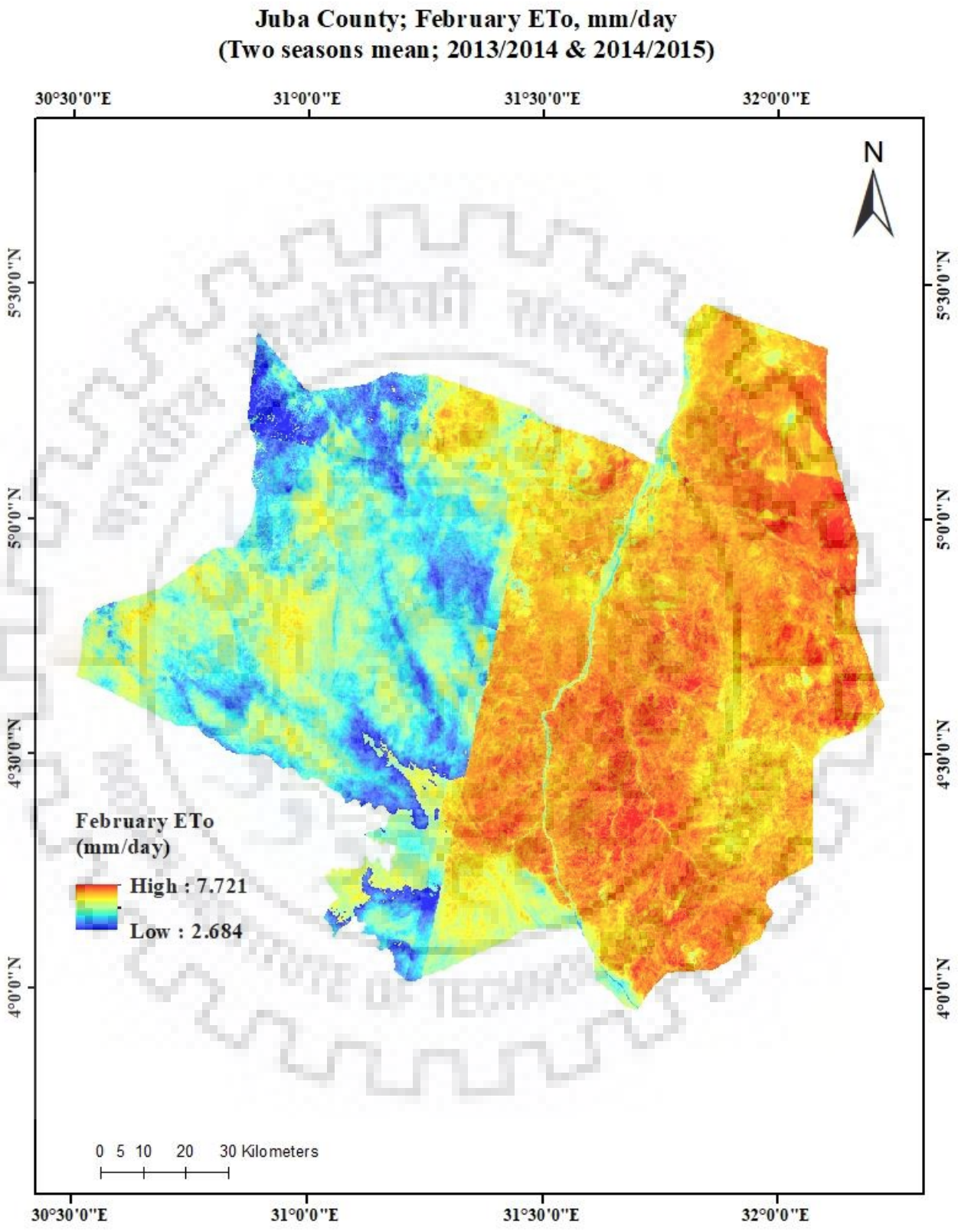

Figure 4. 4: ET_o map of Juba County for the month of February

4.2 LOCATION 2 (ROORKEE, INDIA)

4.2.1 RESULTS

The results for analysis were obtain from a pixel value at same latitude and longitude as one Roorkee's gridded weather station. The monthly results obtained in Rabi season of 2013-2014 (i.e. October 2013 to march 2014 but January exempted because of clouds contamination of satellite images), before models' calibration are presented in table 4.11 and their deviations (errors) from standard FAO-PM values, in percent and in mm/day are shown in tables 4.12 and 4.13 respectively. It can be seen from tables: 4.12 and 4.13 that, only Hargreaves (1985) MODIS based and Thornthwaite (both Landsat and MODIS based) models produced low errors, within a range of less or equal 20% deviation (<= 0.69mm/day) before calibration while other models deviate greatly from standard. Table 4.14 shows the error and regression analysis results and regression lines are presented in figure 4.5 and is observed from the same figure that, Thornthwaite MODIS based, Kharrufa MODIS based and Blaney-criddle MODIS based models shown a best fit than the rest with R^2 of 0.92, 0.92 and 0.90, RMSE of 0.1530, 0.1562 and 0.1761 and MAE of 0.1373, 0.1375, and 0.1327 mm/day respectively. While the other models showed average performance. The satellite based ET_o models' results, after calibration are presented in table 4.15 and their deviation errors are presented in tables 4.16 and 4.17, in percent and mm/day respectively. The monthly errors of all satellite models, after calibration, are within reasonable limit; less than 20% (<0.5mm/day) as illustrated in tables: 4.16 & 4.17.

The calibrated models were validated using three months (October, November and December) of Rabi season of 2014/2015 and the obtained results are tabulated in table 4.18 and monthly errors, in percent and in mm/day are presented in tables 4.19 and 4.20 respectively. It can be observed from tables 4.19 and 4.20 that MODIS based ET_o models exhibited small errors from the validation results, their monthly errors were between 1 to 13% of the standard model's values as shown in figure 4.19. However, the performance of Landsat based ET_o models was also good with R^2 above 0.7, though it's little lower in some cases than MODIS based ET_o models. Thornthwaite, Kharrufa and Blaney-Criddle showed the best fit among Landsat ET_o methods, with R^2 of 0.85, 0.83 and 0.81, RMSE of 0.2173mm/day, 0.2299mm/day & 0.2433mm/day and MAE of 0.1801mm/day, 0.2036mm/day & 0.2178mm/day respectively. Among the best fit Landsat Based ET_o models, Blaney-Criddle was relatively consistent with less monthly errors, all below 25% deviation from standard, while Thornthwaite and Kharrufa produced error of more than 30% deviation from FAO Penman-Montieth ET_o values (table 4.19). Based on regression and error analysis, together with

consideration of spatial resolution of satellite data and sizes of agricultural fields in mind, Blaney-Criddle (Landsat 8 based) was selected and was used to prepared ET_o maps of Roorkee, for three months (October, November and December), average of two Rabi season.

4.2.2 DISCUSSION

In Roorkee, India, before satellite ET_o models calibration, the departure of simulated ET_o values was high (tables: 4.12 & 4.13) and hence calibration was done using standard ET_o values computed by FAO-PM model with station data. Linear regression results showed that the MODIS ET_o models slightly fit better with FAO-PM values than Landsat 8 ET_o models (table 4.6). Nevertheless, little inferior performance of Landsat ET_o models may be because of: (1) atmospheric effect on Landsat 8 images in the season considered (2) error of interpolation of gridded station data which was used in standard FAO-PM model; because no gridded station located in Roorkee region (3) coarse spatial resolution of gridded data used in standard model. Thus, with consideration of agricultural fields scale, high spatial resolution data can be good and so Landsat ET_o models were given a close attention of evaluation.

Thornthwaite, Kharrufa and Blaney-Criddle showed the best fit among Landsat ET_o methods, with R^2 of 0.85, 0.83 and 0.81, RMSE of 0.2173mm/day, 0.2299mm/day & 0.2433mm/day and MAE of 0.1801mm/day, 0.2036mm/day & 0.2178mm/day respectively. And these results are relatively in the same bracket with some results found in different studies, in other places. For instance, Liu, Xu, Zhong, Li, & Yuan, (2017), in a study conducted in China, found R^2 of Blaney-Criddle as 0.804 and RMSE of 1.09mm/day. Also Naorem & Devi, (2014) in a research carried out in Manipur, India, obtained R^2 of 0.51 and 0.63 for Thornthwaite and Blaney-Criddle respectively.

The calibrated LST ET_o models were tested using three months satellite data of different Rabi season rather than one whose data was used in calibration, and it was found that, among the three Landsat ET_o models (Thornthwaite, Kharrufa and Blaney-Criddle) with best fit against FAO PM model, Blaney-Criddle produced low monthly errors and Thornthwaite and Kharrufa give up to 30% deviation error (table 4.19). In table 4.19, it was noticed that three Hargreaves ET_o models based on Lansdsat data produced less monthly errors than Blaney-Criddle but due to the fact that they don't have better R^2s, RMSE and MAE than Blaney-Criddle (see table 4.14), Blaney-Criddle was chosen over them. Blaney-Criddle, Landsat based ET_o model was used to prepare ET_o maps of Roorkee, showing average ET_o values of three months of two Rabi seasons. The maps may help irrigation practitioners in planning. It is worth mentioning here, that the ET_o values depicted in the maps

(figures 4.6, 4.7 & 4.8) are relatively close to historical values reported in some literatures. For example, from maps (figures 4.6, 4.7 & 4.8) the ET_o values of 3.75, 3.03 & 2.82mm/day were obtained at the pixel of central coordinates (29.8543° N, 77.8880° E) of Roorkee, for October, November and December respectively, compare with USA Class A Pan values reported by VARSHNEY et al., (2005), in which the evaporation values for Roorkee station were 3.9, 2.8 and 1.9mm/day for October, November and December respectively.

With the interesting results found in the current study, it can therefore be stated that the proposed methodology may help, in the situation where no ground station data is available, for estimating monthly ET_o values ofr Roorkee region, provide Landsat images are not or less contaminated by clouds.

Table 4. 11: ET_o Models Results before calibration, mm/day (2013-2014)-Roorkee,

Month/Model	Oct	Nov	Dec	Feb	Mar
FAO_PM	3.48	2.88	2.15	2.25	3.39
HargO_ L8 ET_o	5.23	2.99	2.48	3.21	6.02
HargO_Md ET_o	3.41	2.63	1.83	2.68	3.99
HargT_L8 ET_o	4.14	2.43	2.02	2.62	4.75
HargT_Md ET_o	2.88	2.19	1.55	2.25	3.32
HargA_L8 ET_o	2.15	1.29	1.08	1.39	2.47
HargA_Md ET_o	1.53	1.17	0.83	1.2	1.76
HargD_L8 ET_o	2.27	1.29	1.07	1.39	2.61
HargD_Md ET_o	1.48	1.13	0.78	1.15	1.73
BC_L8 ET_o	5.02	3.84	3.59	3.91	5.26
BC_Md ET_o	5.01	3.97	3.34	3.87	4.82
Khar_L8 ET_o	5.45	3.2	2.86	3.13	5.79
Khar_Md ET_o	5.65	3.63	2.45	3.19	4.92
Thw_L8 ET_o	4.00	2.71	2.56	2.57	4.08
Thw_Md ET_o	4.13	3.04	2.26	2.63	3.56

Table 4. 12: Monthly percent error of different models before calibration. (Season 2013/2014)-Roorkee

Month/ET_o model	Deviation of different satellite LST ETo model before calibration, in percent				
	October	November	December	February	March
HargO L8 er	50%	4%	15%	43%	78%
hargO Md er	-2%	-9%	-15%	19%	18%
HargT L8 er	19%	-16%	-6%	16%	40%
HargT Md er	-17%	-24%	-28%	0%	-2%
HargA L8 er	-38%	-55%	-50%	-38%	-27%
HgA Md er	-56%	-59%	-61%	-47%	-48%
HgD L8 er	-35%	-55%	-50%	-38%	-23%
HgD Md er	-57%	-61%	-64%	-49%	-49%
BC L8 er	44%	33%	67%	74%	55%
BC Md er	44%	38%	55%	72%	42%
Kharr L8 er	57%	11%	33%	39%	71%
Kharr Md er	62%	26%	14%	42%	45%
Thw L8 er	15%	-6%	19%	14%	20%
Thw Md er	19%	6%	5%	17%	5%

Table 4. 13: Monthly ETo error of different models before calibration, in mm/day (season 2013/2014) -Roorkee

Month/ETo model	Deviation of different satellite LST ETo model before calibration, in mm/day				
	October	November	December	February	March
HargO L8 er	1.75	0.11	0.33	0.96	2.63
hargO Md er	-0.07	-0.25	-0.32	0.43	0.6
HargT L8 er	0.66	-0.45	-0.13	0.37	1.36
HargT Md er	-0.6	-0.69	-0.6	0	-0.07
HargA L8 er	-1.33	-1.59	-1.07	-0.86	-0.92
HgA Md er	-1.95	-1.71	-1.32	-1.05	-1.63
HgD L8 er	-1.21	-1.59	-1.08	-0.86	-0.78
HgD Md er	-2	-1.75	-1.37	-1.1	-1.66
BC L8 er	1.54	0.96	1.44	1.66	1.87
BC Md er	1.53	1.09	1.19	1.62	1.43
Kharr L8 er	1.97	0.32	0.71	0.88	2.4
Kharr Md er	2.17	0.75	0.3	0.94	1.53
Thw L8 er	0.52	-0.17	0.41	0.32	0.69
Thw Md er	0.65	0.16	0.11	0.38	0.17

Table 4. 14: Summary of regression and overall error analysis (2013-2014)-Roorkee

Evaluation indicator/ model		R^2	R	RSME Mm/day	MAE Mm/day	Developed regression equations Y= dependent variable X= ET_o estimated from satellite data
BC	Landsat 8	0.81	0.90	0.2433	0.2178	Y = 0.7339X - 0.3434
	MODIS	0.90	0.95	0.1761	0.1327	Y = 0.8437X - 0.7153
HargO	Landsat 8	0.77	0.88	0.2632	0.2450	Y = 0.3532X + 1.4221
	MODIS	0.76	0.87	0.2703	0.2325	Y = 0.6572X + 0.919
HargT	Landsat 8	0.77	0.88	0.2649	0.2458	Y = 0.46X + 1.3618
	MODIS	0.77	0.88	0.2669	0.2293	Y = 0.7972X + 0.8865
HargD	Landsat 8	0.77	0.88	0.2637	0.2450	Y = 0.8106X + 1.4309
	MODIS	0.77	0.88	0.2672	0.2304	Y = 1.4946X + 0.9558
HargA	Landsat 8	0.77	0.88	0.2670	0.2482	Y = 0.9053X + 1.3128
	MODIS	0.77	0.88	0.2665	0.2292	Y = 1.5191X + 0.8582
Kharr.	Landsat 8	0.83	0.91	0.2299	0.2036	Y = 0.3998X + 1.1965
	MODIS	0.92	0.96	0.1562	0.1375	Y = 0.4576X + 1.0243
Thw	Landsat 8	0.85	0.92	0.2173	0.1801	Y = 0.7248X + 0.5228
	MODIS	0.92	0.96	0.1530	0.1373	Y = 0.8029X + 0.321

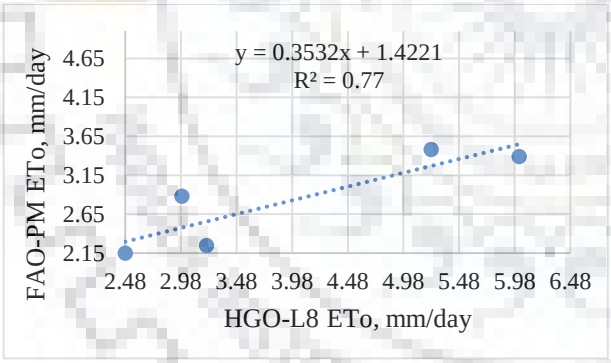

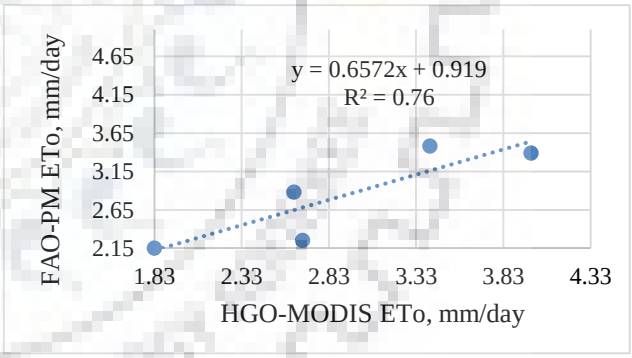

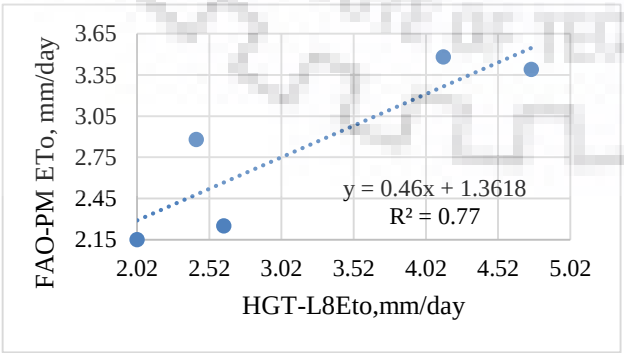

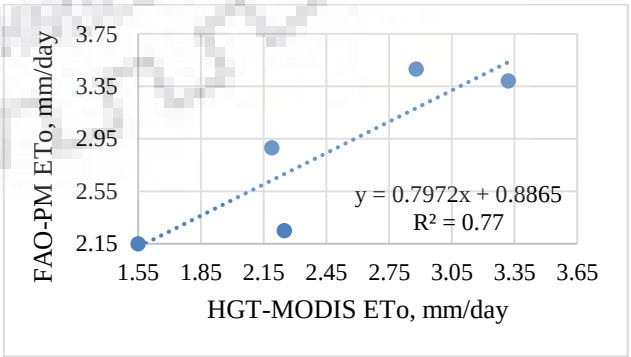

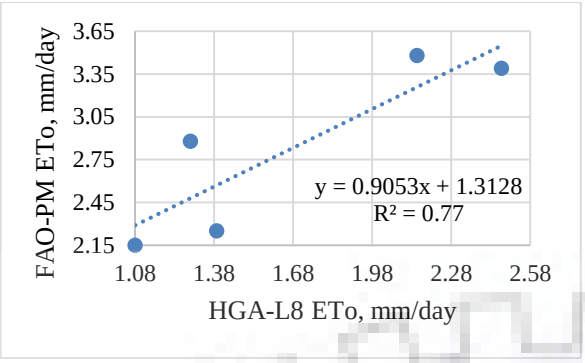
FAO-PM ETo, mm/day
3.65
3.35
3.05
2.75
2.45
2.15
y = 0.9053x + 1.3128
R² = 0.77
1.08 1.38 1.68 1.98 2.28 2.58
HGA-L8 ETo, mm/day

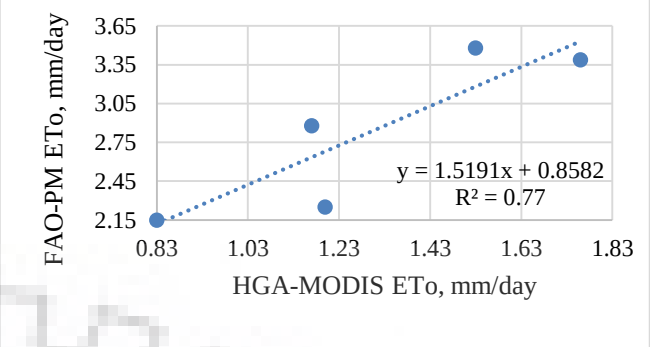
FAO-PM ETo, mm/day
3.65
3.35
3.05
2.75
2.45
2.15
y = 1.5191x + 0.8582
R² = 0.77
0.83 1.03 1.23 1.43 1.63 1.83
HGA-MODIS ETo, mm/day

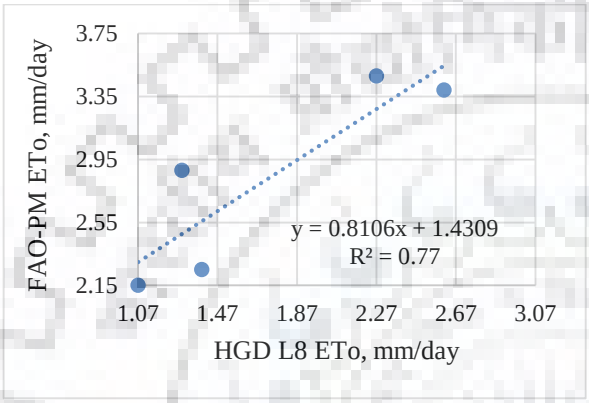
FAO-PM ETo, mm/day
3.75
3.35
2.95
2.55
2.15
y = 0.8106x + 1.4309
R² = 0.77
1.07 1.47 1.87 2.27 2.67 3.07
HGD L8 ETo, mm/day

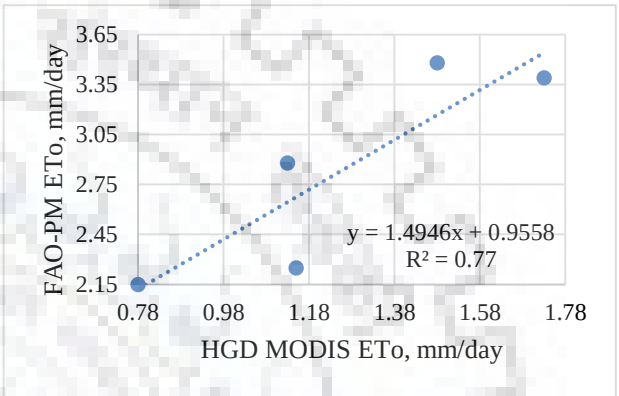
FAO-PM ETo, mm/day
3.65
3.35
3.05
2.75
2.45
2.15
y = 1.4946x + 0.9558
R² = 0.77
0.78 0.98 1.18 1.38 1.58 1.78
HGD MODIS ETo, mm/day

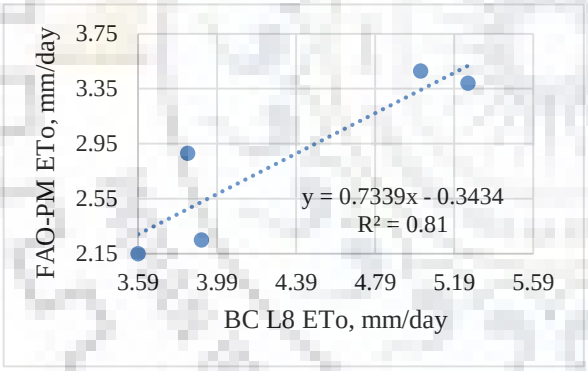
FAO-PM ETo, mm/day
3.75
3.35
2.95
2.55
2.15
y = 0.7339x - 0.3434
R² = 0.81
3.59 3.99 4.39 4.79 5.19 5.59
BC L8 ETo, mm/day

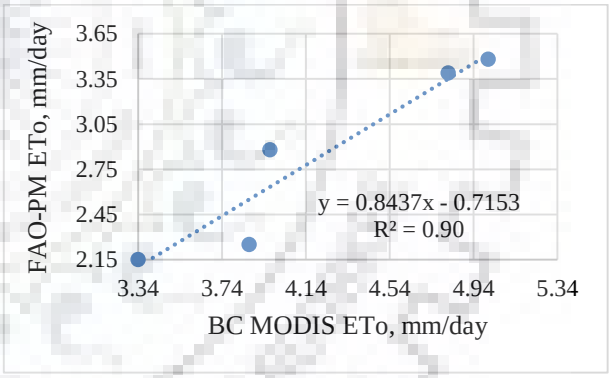
FAO-PM ETo, mm/day
3.65
3.35
3.05
2.75
2.45
2.15
y = 0.8437x - 0.7153
R² = 0.90
3.34 3.74 4.14 4.54 4.94 5.34
BC MODIS ETo, mm/day

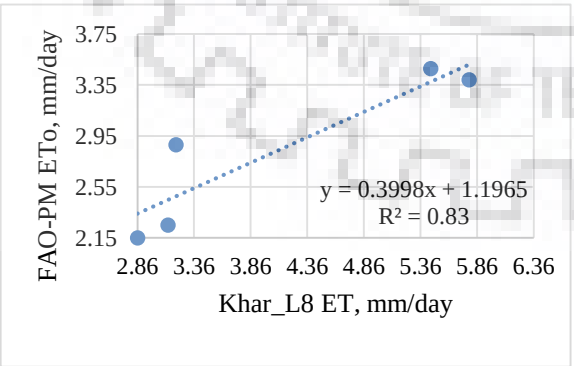
FAO-PM ETo, mm/day
3.75
3.35
2.95
2.55
2.15
y = 0.3998x + 1.1965
R² = 0.83
2.86 3.36 3.86 4.36 4.86 5.36 5.86 6.36
Khar_L8 ET, mm/day

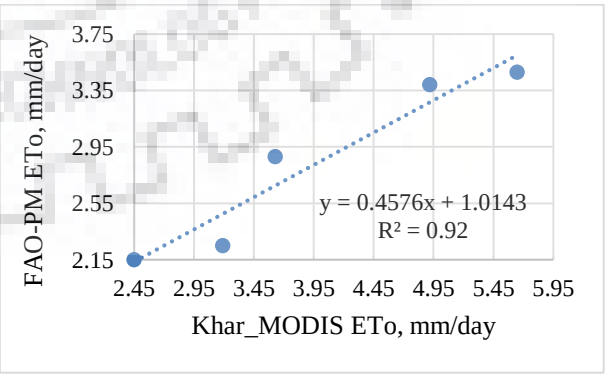
FAO-PM ETo, mm/day
3.75
3.35
2.95
2.55
2.15
y = 0.4576x + 1.0143
R² = 0.92
2.45 2.95 3.45 3.95 4.45 4.95 5.45 5.95
Khar_MODIS ETo, mm/day

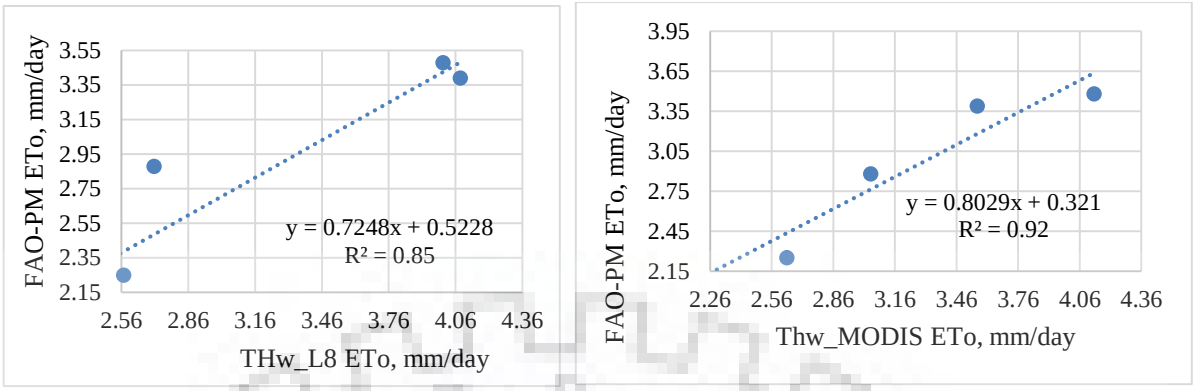

Figure 4. 5: Regression graphs using different satellite data-Roorkee

Table 4. 15: ETo Models Results after calibration (2013-2014), in mm/day-Roorkee

Month/Model	October	November	December	February	March
FAO-PM	3.48	2.88	2.15	2.25	3.39
HargO L 8 ET_o	3.27	2.48	2.30	2.56	3.55
HargO Md ET_o	3.16	2.65	2.12	2.68	3.54
HargT L 8 ET_o	3.27	2.48	2.29	2.57	3.55
HargT Md ET_o	3.18	2.63	2.12	2.68	3.53
HargA L 8 ET_o	3.26	2.48	2.29	2.57	3.55
HargA Md ET_o	3.18	2.64	2.12	2.68	3.53
HargD L 8 ET_o	3.27	2.48	2.30	2.56	3.55
HargD Md ET_o	3.17	2.64	2.12	2.67	3.54
BC L 8 ET_o	3.34	2.47	2.29	2.53	3.52
BC Md ET_o	3.51	2.63	2.10	2.55	3.35
Kharr L 8 ET_o	3.38	2.48	2.34	2.45	3.51
Kharr Md ET_o	3.60	2.68	2.14	2.47	3.27
Thw L 8 ET_o	3.42	2.48	2.37	2.39	3.48
Thw Md ET_o	3.64	2.76	2.13	2.44	3.18

Table 4. 16: Monthly percent errors of different Models after calibration, mm/day (season 2013/2014) -Roorkee

Month/ET_o Model	Deviation of different satellite LST ETo model before calibration, in percent				
	October	November	December	February	March
BC L8 er	-4%	-14%	7%	12%	4%
BC Md er	1%	-9%	-2%	13%	-1%
HargO L8 er	-6%	-14%	7%	14%	5%
HargO Md er	-9%	-8%	-1%	19%	4%
HargT L8 er	-6%	-14%	7%	14%	5%
HargT Md er	-9%	-9%	-1%	19%	4%
HargD L8 er	-6%	-14%	7%	14%	5%
HargD Md er	-9%	-8%	-1%	19%	4%
HargA L8 er	-6%	-14%	7%	14%	5%
HargA Md er	-9%	-8%	-1%	19%	4%
Khar L8 er	-3%	-14%	9%	9%	4%
Khar Md er	3%	-7%	-1%	10%	-4%
Thw L8 er	-2%	-14%	10%	6%	3%
Thw Md er	5%	-4%	-1%	8%	-6%

Table 4. 17: Monthly ET_o error of different Models after calibration, in mm/day-Roorkee (season 2013/2014)

Month/ETo Model	Deviation of different satellite LST ETo model before calibration, in mm/day				
	October	November	December	February	March
BC L8 er	-0.139	-0.405	0.141	0.276	0.127
BC Md er	0.032	-0.246	-0.047	0.300	-0.039
HargO L8 er	-0.211	-0.402	0.148	0.306	0.158
HargO Md er	-0.320	-0.233	-0.028	0.430	0.151
HargT L8 er	-0.214	-0.400	0.141	0.317	0.157
HargT Md er	-0.298	-0.248	-0.028	0.430	0.143
HargD L8 er	-0.209	-0.403	0.148	0.308	0.157
HargD Md er	-0.312	-0.235	-0.028	0.425	0.151
HargA L8 er	-0.221	-0.399	0.141	0.321	0.159
HargA Md er	-0.298	-0.244	-0.031	0.431	0.142
Khar L8 er	-0.105	-0.404	0.190	0.198	0.121

Khar Md er	0.120	-0.205	-0.015	0.224	-0.124
Thw L8 er	-0.055	-0.395	0.225	0.135	0.090
Thw Md er	0.157	-0.116	-0.018	0.186	-0.210

Table 4. 18: ETo Models out-of-time validation Results (2014-2015), mm/day-Roorkee

Month/Model	October	November	December
FAO-PM ET_o	3.70	3.00	1.92
HargO_L8 ET_o	3.09	2.47	2.22
HargO_Md ET_o	3.26	2.63	2.05
HargT_L8 ET_o	3.09	2.47	2.21
HargT_Md ET_o	3.27	2.62	2.06
HargA_L8 ET_o	3.09	2.47	2.21
HargA_Md ET_o	3.27	2.62	2.07
HargD_L8 ET_o	3.09	2.46	2.22
HargD_Md ET_o	3.26	2.63	2.06
BC_L8 ET_o	2.88	2.46	2.17
BC_Md ET_o	3.56	2.63	2.04
Khar_L8 ET_o	2.56	2.46	2.20
Khar_Md ET_o	3.67	2.67	2.07
Thw_L8 ET_o	2.56	2.07	1.85
Thw_Md ET_o	3.44	2.65	2.01

Table 4. 19: Monthly ETo percent errors of different Models for out-of-time validation, in mm/day (season 2014/2015) - Roorkee

	Deviation of different satellite LST ETo model before calibration, in percent		
Month/ETo Model	October	November	December
HargO_L8 er	-16%	-18%	16%
HargO_Md er	-12%	-12%	7%
HargT_L8 er	-16%	-18%	15%
HargT_Md er	-12%	-13%	7%

HargA_L8 er	-16%	-18%	15%
HargA_Md er	-12%	-13%	8%
HargD_L8 er	-16%	-18%	16%
HargD_Md er	-12%	-12%	7%
BC_L8 er	-22%	-18%	13%
BC_Md er	-4%	-12%	6%
Khar_L8 er	-31%	-18%	15%
Khar_Md er	-1%	-11%	8%
Thw_L8 er	-31%	-31%	-4%
Thw_Md er	-7%	-12%	5%

Table 4. 20: Monthly ETo errors of different Models for out-of-time validation, in mm/day (season 2014/2015) -Roorkee

	Deviation of different satellite LST ETo model before calibration, in mm/day		
Month/ETo Model	October	November	December
HargO_L8 er	-0.61	-0.53	0.3
HargO_Md er	-0.44	-0.37	0.13
HargT_L8 er	-0.61	-0.53	0.29
HargT_Md er	-0.43	-0.38	0.14
HargA_L8 er	-0.61	-0.53	0.29
HargA_Md er	-0.43	-0.38	0.15
HargD_L8 er	-0.61	-0.54	0.3
HargD_Md er	-0.44	-0.37	0.14
BC_L8 er	-0.82	-0.54	0.25
BC_Md er	-0.14	-0.37	0.12
Khar_L8 er	-1.14	-0.54	0.28
Khar_Md er	-0.03	-0.33	0.15
Thw_L8 er	-1.14	-0.93	-0.07
Thw_Md er	-0.26	-0.35	0.09

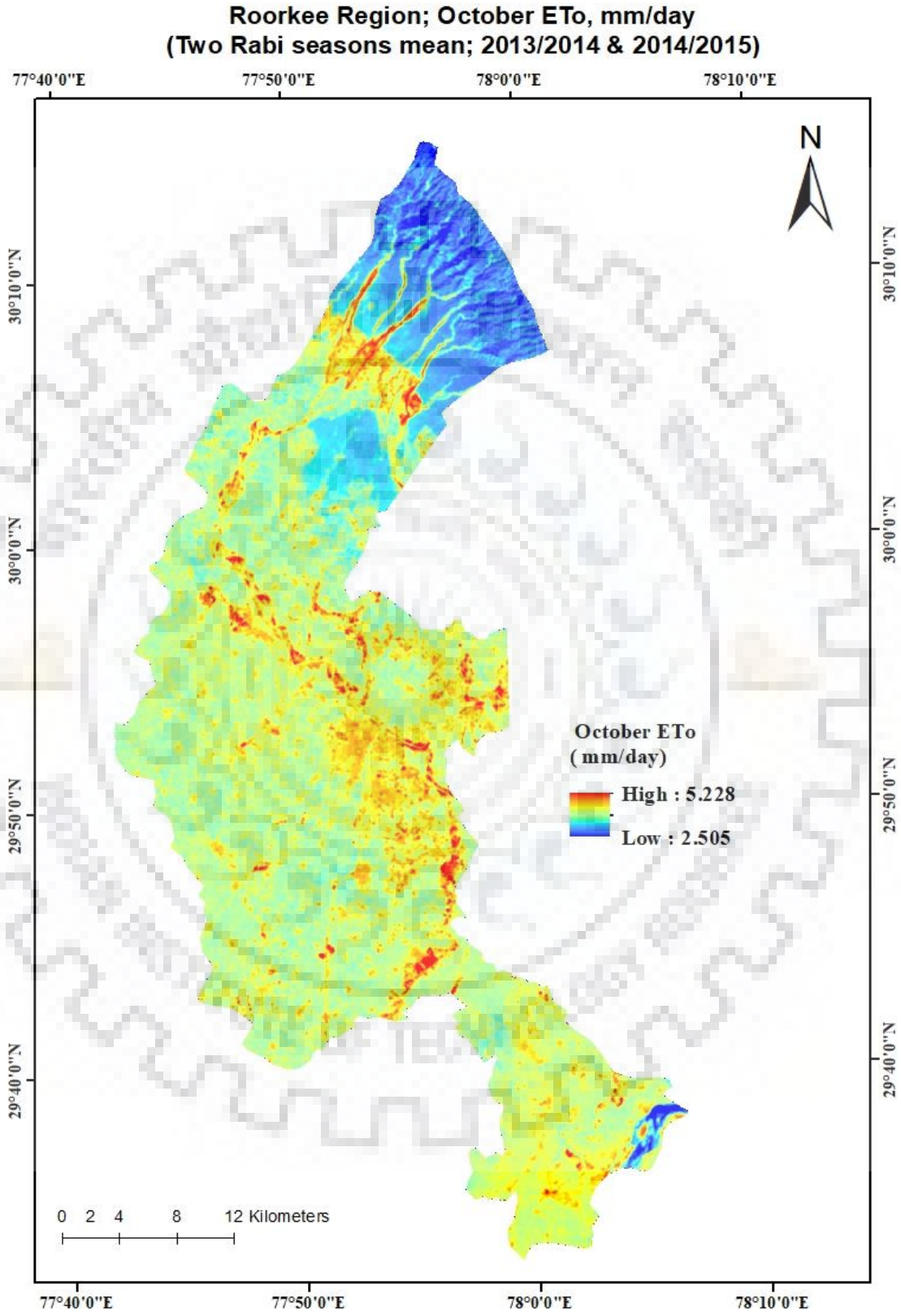

Figure 4. 6: ETo map of Roorkee for the month of October

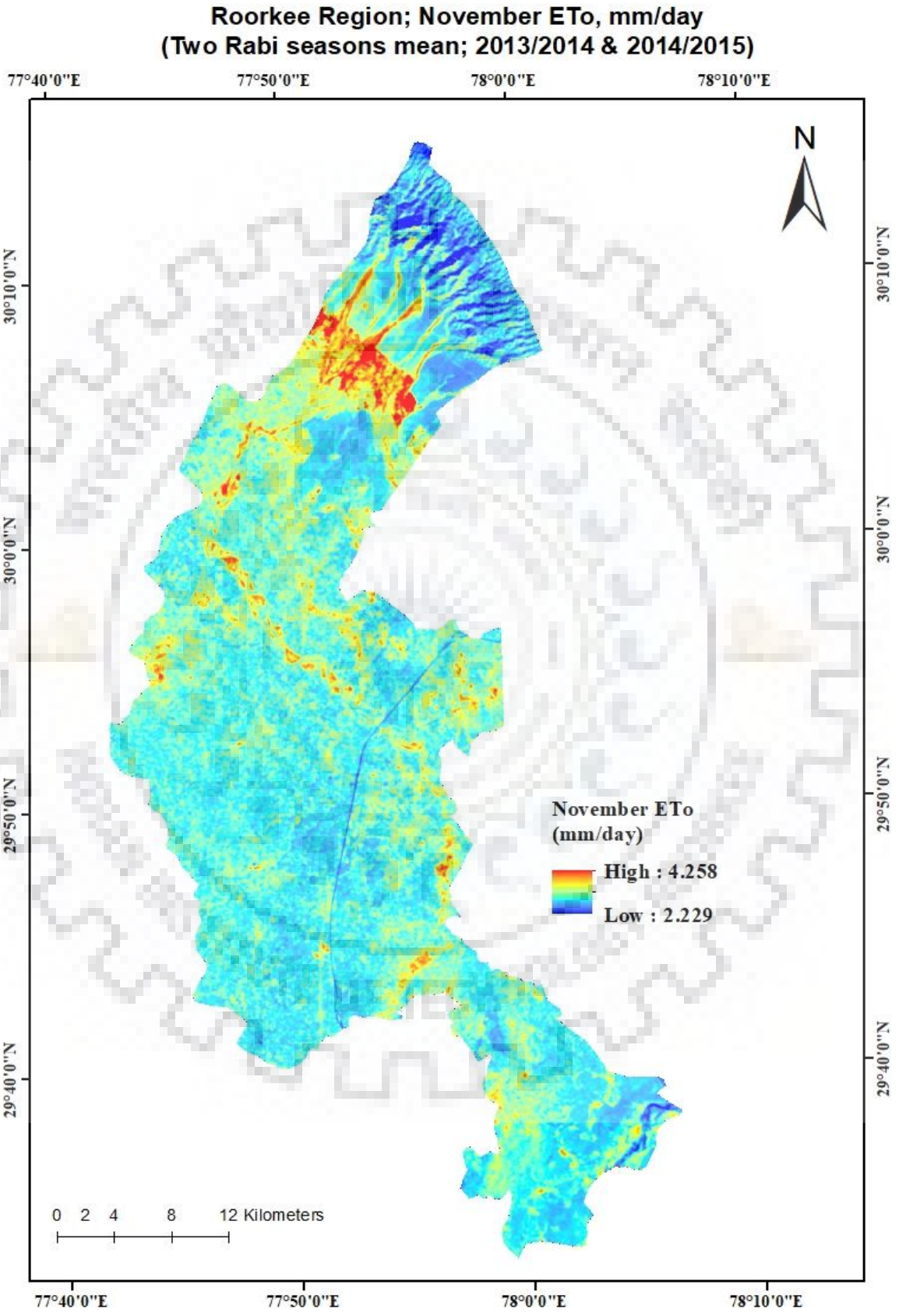

Figure 4. 7: ETo map of Roorkee for the month of November

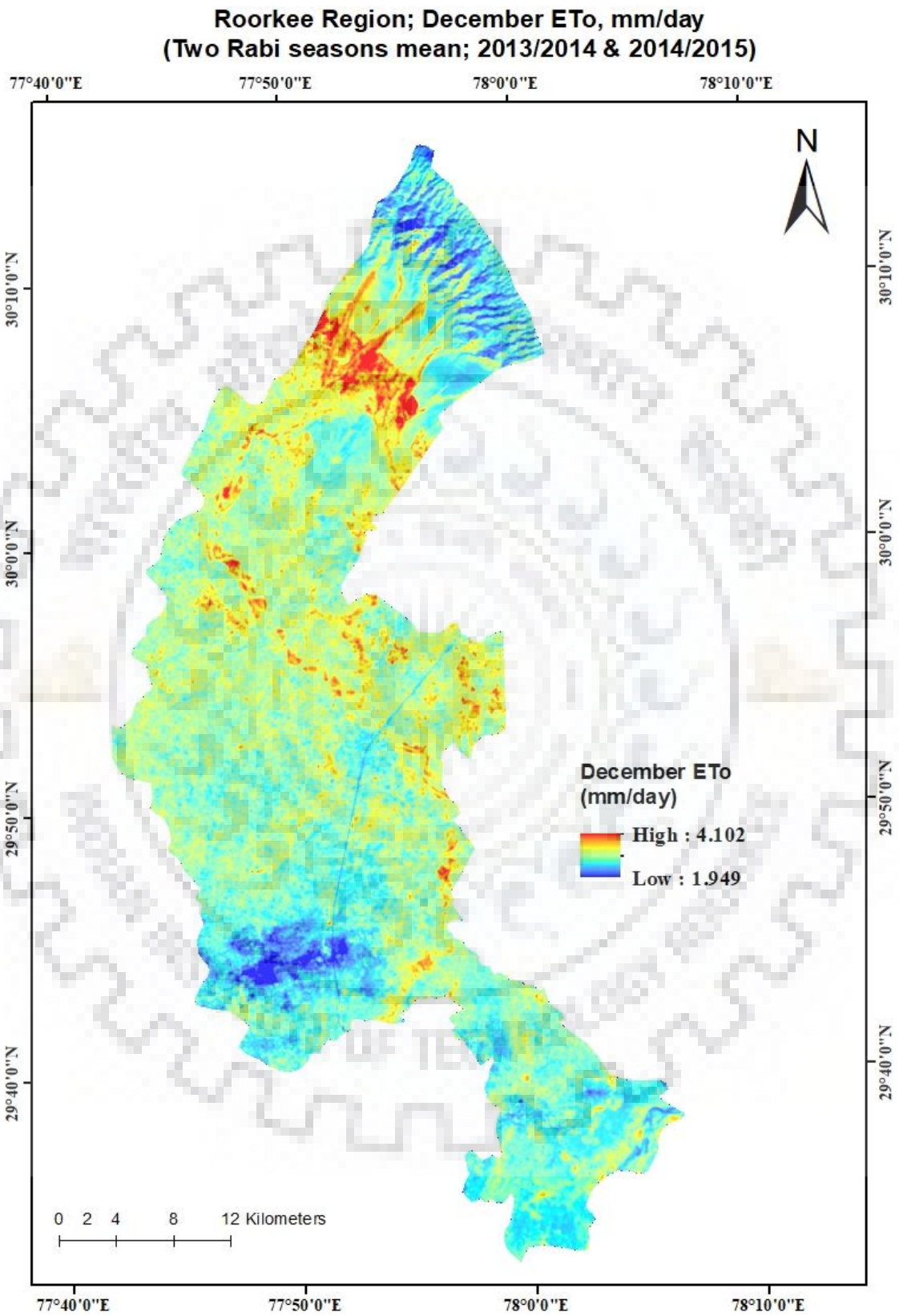

Figure 4. 8: ETo map of Roorkee for the month of December

CHAPTER V

SUMMARY AND CONCLUSION.

5.1 SUMMARY

Reference crop evapotranspiration (ET_o) data is very important in irrigation and many other water consuming sectors. However, direct measurement or getting required data for indirect estimation of ET_o is cumbersome. Emergence of remote sensing technology, for recording earth surface features response to solar radiation (which is the principle driver of ET_o) opened avenues in solving the difficulty in getting ET_o data. Many remote sensing techniques have been developed over the past years for ET_o estimation but less or no techniques that produce ET_o without involving measured data from ground surface station.

This study was conducted in two areas: Juba County in South Sudan which cover an area of about 18789 km^2 and Roorkee region in India which is stretched over an area of about 1187.2 km^2. The study has been done to evaluate the possibility of estimating monthly ET_o values without station data, by employing seven commonly used temperature based ET_o models (Thornthwaite, Blaney-criddle, Kharrufa (1985), Hargreaves (1985), Droogers et al. (2002) modified Hargreaves, Allen et al. (1993) modified Hargreaves and Trajkovic (2007) modified Hargreaves methods), parameterized with LST derived from satellite remote sensing data, instead of conventional air temperature. Two satellites remote sensing LST were used; Landsat 8 LST and MODIS LST. Satellite image processing models were built in ArcGIS, based on the selected ET_o methods to automatically extract ET_o values from satellite images.

The Monthly ET_o was estimated in one season, using Landsat 8 LST and MODIS LST, differently, in each of the study areas; it was dry season (November to March) in case of Juba County and Rabi season (October to March) in case of Roorkee. FAO Penman Montieth model was used, with station data, for calibration and validation.

In Juba County, South Sudan, results has shown that ET_o models parameterized with Landsat 8 LST have better relationship with FAO PM model than MODIS LST based models; their R^2 were all, over 0.9 in all months, in a season. And Hargreaves (Landsat based) ET_o produced the best results in Juba County, R^2=0.93, RMSE=0.1064mm/day and MAE=0.0163mm/day and thus, may be used in this area for ET_o estimation.

In Roorkee, India, results revealed that both Landsat and MODIS ET_o models have good relationship with FAO PM Model; R^2 was over 0.7 for all. Thornthwaite, Kharrufa and Blaney-Criddle produced

good results than the rest, their R^2s were 0.92, 0.92 & 0.9 respectively, when based on MODIS LST and 0.85, 0.83 & 0.81 respectively when based on Landsat LST. Considering spatial resolution of different satellite data together with model performance and small size of agricultural fields, Blaney-Criddle based on Landsat LST was found as good for Roorkee region. It produced reasonable monthly errors (less than 25%) in both calibration and validation. Unlike Thornthwaite and Kharrufa (Landsat based) models, which in some months, during validation produced errors more than 30%.

Finally spatial ET_o maps for the two study areas were prepared using (1) Hargreaves Landsat LST ET_o model for Juba County. (2) Blaney-Criddle Landsat LST ET_o model for Roorkee.

5.2 CONCLUSION

The following conclusion can be drawn from this study:

[1] In Juba County, South Sudan, Landsat ET_o models performed better than MODIS ET_o models with $R^2 = 0.9$. Hargreaves original model (Landsat 8 based) was the best ($R^2 = 0.93$) and produces errors less than any other model, in both cases, during calibration and validation.

[2] In Roorkee region, the performance of empirical models based on Landsat data was slightly lower than MODIS ET_o but also good, R^2 was above 0.7. Blaney-Criddle showed relatively good (R^2 of 0.81 and deviation errors below 25%) performance among Landsat ET_o models, it produced minimum monthly errors, both during calibration and validation.

[3] Average performance of Landsat based empirical models in Roorkee region, India is assumed due to: (1) atmospheric effect on Landsat 8 images in the season considered (2) error of interpolation of gridded station data which was used in standard FAO-PM model; because no gridded station located in Roorkee region (3) coarse spatial resolution of gridded data used in standard model.

[4] Spatial ET_o maps may help planners for spatial for irrigation management.

[5] The satellite image processing models developed in this study can help in quickening of the complex processing steps in computation of ET_o from satellite images.

Landsat 8 data can be freely downloaded from internet with high spatial resolution of 30m and 16 day temporal resolution, hence the proposed procedure can be helpful in estimating ET_o even at smaller field scale, considering the resolution and can assists, when no station data available, in planning and management of irrigation systems in the study areas.

LIMITATIONS

The proposed ET_o methodology is affected by clouds contamination of satellite images and hence not advisable in clouds frequented locations or months prone to clouds cover.

The methodology may not be applied in locations where weather conditions vary greatly within a month. Because the method assumed that, there is very small variation of weather parameters within a month. If weather conditions vary greatly within a month, then result will be erroneous.

FUTURE WORKS TO BE TRIED

[1] Disaggregated MODIS LST into high spatial resolution using Landsat or Sentinel 2 visible and near infrared (VNIR) data should be tried in future, in the proposed methodology, to see whether it can improve temporal as well as spatial resolution. Many LST disaggregation methods are there, for instance thermal sharpening (TSP) and temperature unmixing LST disaggregation methods(TUM) (X. Li et al., 2017)

[2] The proposed methodology in this study should be done in actual agricultural field(s) since the current work was conducted at regional scale, without any crop field singled out.

[3] Many weather variables that were involved in computing reference ET_o values were derived from air temperatures by Cropwat software and it's therefore recommended that full measured station datasets must be used in the suggested future work when shorter times are considered.

LIST OF PAPERS AND PRESENTATIONS

[1] Samuel Malou Mukpuou, Ashish Pandey and V.M. chowdary, "*REFERENCE CROP EVAPOTRANSPIRATION ESTIMATION USING REMOTE SENSING TECHNIQUE"* presented in the International Conference on Sustainable Technologies for Intelligent water Management, IIT-Roorkee February 2018. And **THE PAPER WON THE FIRST PRIZE PICO AWARD** of the conference on 19th Feb. 2018.

REFERENCES

Allen, R. G., Pereira, L. S., Raes, D., Smith, M., & W, a B. (1998). Crop evapotranspiration - Guidelines for computing crop water requirements - FAO Irrigation and drainage paper 56. *Irrigation and Drainage*, 1–15. https://doi.org/10.1016/j.eja.2010.12.001

Aquastat, F. (2015). http://www.fao.org/nr/water/aquastat/countries_regions/SSD/index.stm.

Avdan, U., & Jovanovska, G. (2016). Algorithm for automated mapping of land surface temperature using LANDSAT 8 satellite data. *Journal of Sensors*, *2016*, 1–8. https://doi.org/10.1155/2016/1480307

Azhar, A. H., & Perera, B. J. C. (2011). Evaluation of Reference Evapotranspiration Estimation Methods under Southeast Australian Conditions. *Irrigation and Drainage Engineering*, *137*(May), 268–279. https://doi.org/10.1061/(ASCE)IR.1943-4774.0000297.

Bajirao, T. S., & Awari, H. W. (2017). Estimation of reference evapotranspiration for Parbhani district, *10*(1), 51–54. https://doi.org/10.15740/HAS/IJAE/10.1/51-54

Bois, B., Pieri, P., Van Leeuwen, C., Wald, L., Huard, F., Gaudillere, J. P., & Saur, E. (2008). Using remotely sensed solar radiation data for reference evapotranspiration estimation at a daily time step. *Agricultural and Forest Meteorology*, *148*(4), 619–630. https://doi.org/10.1016/j.agrformet.2007.11.005

Carlson, T. C., & Ripley, D. a. (1997). On the relationship between NDVI, fractional vegetation cover, and leaf area index. *Remote Sensing of Environment*, *62*, 241–252. https://doi.org/10.1016/S0034-4257(97)00104-1

Dile, Y. T., & Srinivasan, R. (2014). EVALUATION OF CFSR CLIMATE DATA FOR HYDROLOGIC PREDICTION IN DATA- SCARCE WATERSHEDS : AN APPLICATION IN THE BLUE NILE RIVER BASIN 1, *77845*. https://doi.org/10.1111/jawr.12182

Doorenbos, J., & Pruitt, W. O. (1977). Guidelines for predicting crop water requirements. *FAO Irrigation and Drainage Paper*, *24*, 144.

Douglas, E. M., Jacobs, J. M., Sumner, D. M., & Ray, R. L. (2009). A comparison of models for estimating potential evapotranspiration for Florida land cover types. *Journal of Hydrology*, *373*(3–4), 366–376. https://doi.org/10.1016/j.jhydrol.2009.04.029

Droogers, P., & Allen, R. G. (2002). Estimating reference evapotranspiration under. *Irrigation and Drainage Systems*, *16*, 33–45. https://doi.org/10.1023/A:1015508322413

Efthimiou, N., Alexandris, S., Karavitis, C., & Mamassis, N. (2013). Comparative analysis of reference evapotranspiration estimation between various methods and the FAO56 Penman - Monteith procedure, 19–34.

El-Shirbeny, M. A. (2016). Evaluation of Hargreaves Based on Remote Sensing Method To Estimate Potential Crop Evapotranspiration. *International Journal of Geomate*, *11*(23), 2143–2149. https://doi.org/10.21660/2016.23.1122

Fooladmand, H. R., Zandilak, H., & Ravanan, M. H. (2008). Comparison of different types of Hargreaves equation for estimating monthly evapotranspiration in the south of Iran. *Archives of Agronomy and Soil Science*, *54*(3), 321–330. https://doi.org/10.1080/03650340701793603

Fuka, D. R., Walter, M. T., Macalister, C., Degaetano, A. T., Steenhuis, T. S., & Easton, Z. M. (2013). Using the Climate Forecast System Reanalysis as weather input data for watershed models. https://doi.org/10.1002/hyp.10073

Garg, S. K. (2006). *Chapter 19 - Design and Construction of Gravity Dams*. *Irrigation Engineering and*

Hydraulic Structures.

George H. Hargreaves, & Zohrab A. Samani. (1985). Reference Crop Evapotranspiration from Temperature. *Applied Engineering in Agriculture*. https://doi.org/10.13031/2013.26773

Giannini, M. B., Belfiore, O. R., Parente, C., & Santamaria, R. (2015). *Land Surface Temperature from Landsat 5 TM images: Comparison of different methods using airborne thermal data*. *Journal of Engineering Science and Technology Review* (Vol. 8). https://doi.org/10.1007/s00024-013-0685-7

GOSS, M. I. D. M. P., (IDMP), SUDAN, I. T. R. O. S., REPORT, F., & (MAIN). (2015). *Irrigation Development Master Plan Report*. Retrieved from http://open_jicareport.jica.go.jp/pdf/12249181.pdf

Granger, R. J. (2000). Satellite-derived estimates of evapotranspiration in the Gediz basin. *Journal of Hydrology*, *229*(1–2), 70–76. https://doi.org/10.1016/S0022-1694(99)00200-0

Hess, T. M., & White, S. M. (2009). ESTIMATION OF REFERENCE EVAPOTRANSPIRATION IN A MOUNTAINOUS MEDITERRANEAN SITE USING THE PENMAN-MONTEITH EQUATION WITH LIMITED METEOROLOGICAL DATA, 7–31.

Heydari, M. M., Aghamajidi, R., Beygipoor, G., & Heydari, M. (2014). 38 EQUATIONS FOR ESTIMATING REFERENCE, *23*(8), 1985–1996.

Hosseinzadeh Talaee, P. (2014). Performance evaluation of modified versions of Hargreaves equation across a wide range of Iranian climates. *Meteorology and Atmospheric Physics*, *126*(1–2), 65–70. https://doi.org/10.1007/s00703-014-0333-5

Issn, A. E., & Estadual, U. (2016). Comparison of methods for estimating reference evapotranspiration: an approach to the management of water resources within an experimental basin in the brazilian cerrado, *4430*, 1016–1026.

Kamble, B., Kilic, A., & Hubbard, K. (2013). Estimating crop coefficients using remote sensing-based vegetation index. *Remote Sensing*, *5*(4), 1588–1602. https://doi.org/10.3390/rs5041588

Kisi, O. (2013). Irrigation & Drainage Systems Engineering Estimation of Reference Evapotranspiration : Need for Generalized Models, *2*(1), 9768. https://doi.org/10.4172/2168-9768.1000e116

Kustas, W. P., Norman, J. M., Anderson, M. C., & French, A. N. (2003). Estimating subpixel surface temperatures and energy fluxes from the vegetation index – radiometric temperature relationship, *85*, 429–440. https://doi.org/10.1016/S0034-4257(03)00036-1

Landsat 8, data U. H. (2016). Landsat 8 (L8) Data Users Handbook. *America*, *8*(1993), 1993–1993. https://doi.org/http://www.webcitation.org/6mu9r7riR

Lanjeri, S. (2007). Comparison of different procedures to map reference evapotranspiration using geographical information systems and regression-based techniques, *1118*(February), 1103–1118. https://doi.org/10.1002/joc

Li, H., Zheng, L., Lei, Y., Li, C., Liu, Z., & Zhang, S. (2008). Estimation of water consumption and crop water productivity of winter wheat in North China Plain using remote sensing technology, *95*, 1271–1278. https://doi.org/10.1016/j.agwat.2008.05.003

Li, R., Min, Q., & Lin, B. (2018). Remote Sensing of Environment Estimation of evapotranspiration in a mid-latitude forest using the Microwave Emissivity Difference Vegetation Index (EDVI). *Remote Sensing of Environment*, *113*(9), 2011–2018. https://doi.org/10.1016/j.rse.2009.05.007

Li, X., Xin, X., Jiao, J., Peng, Z., Zhang, H., Shao, S., & Liu, Q. (2017). Estimating Subpixel Surface Heat Fluxes through Applying Temperature-Sharpening Methods to MODIS Data. https://doi.org/10.3390/rs9080836

Liou, Y., & Kar, S. K. (2014). Evapotranspiration Estimation with Remote Sensing and Various Surface Energy Balance Algorithms—A Review, 2821–2849. https://doi.org/10.3390/en7052821

Liu, X., Xu, C., Zhong, X., Li, Y., & Yuan, X. (2017). Comparison of 16 models for reference crop evapotranspiration against weighing lysimeter measurement. *Agricultural Water Management*, *184*, 145–155. https://doi.org/10.1016/j.agwat.2017.01.017

Maeda, E. E., Wiberg, D. A., & Pellikka, P. K. E. (2011). Estimating reference evapotranspiration using remote sensing and empirical models in a region with limited ground data availability in Kenya. *Applied Geography*, *31*(1), 251–258. https://doi.org/10.1016/j.apgeog.2010.05.011

Montes, C., Jacob, F., & Member, S. (2017). Comparing Landsat-7 ETM + and ASTER Imageries to Estimate Daily Evapotranspiration Within a Mediterranean Vineyard Watershed, *14*(3), 459–463.

Naorem, N., & Devi, T. K. (2014). Estimation of Potential Evapotranspiration using Empirical Models for Imphal, (7).

Othoman ALKAEED *, Clariza FLORES **, K. J. and A. T. (2006). Comparison of Several Reference Evapotranspiration Methods for Itoshima Peninsula Area, Fukuoka, Japan by Othoman ALKAEED *, Clariza FLORES **, Kenji JINNO*** and Atsushi TSUTSUMI****, *66*(1), 1–14.

Pandey, P. K., Dabral, P. P., & Pandey, V. (2016). International Soil and Water Conservation Research Evaluation of reference evapotranspiration methods for the northeastern region of India. *International Soil and Water Conservation Research*, *4*(1), 52–63. https://doi.org/10.1016/j.iswcr.2016.02.003

Papadavid, G., Hadjimitsis, D., Michaelides, S., & Nisantzi, A. (2011). Advances in Geosciences Crop evapotranspiration estimation using remote sensing and the existing network of meteorological stations in Cyprus, (2001), 39–44. https://doi.org/10.5194/adgeo-30-39-2011

R.S. VARSHNEY, S. C. G. A. R. L. G. (2005). *THEORY AND DESIGN OF IRRIGATION STRUCTURES*. Nem Chand & Bros Civil Lnes, Roorkee 247667 INDIA.

Rao, B. B., Sandeep, V. M., & Venkateswarlu, B. (2012). Potential Evapotranspiration estimation for Indian conditions : Improving accuracy through calibration coefficients, 1–60.

Ray, S. ., & Dadhwal, V. . (2001). Estimation of crop evapotranspiration of irrigation command area using remote sensing and GIS. *Agricultural Water Management*, *49*, 239–249. https://doi.org/10.1016/S0378-3774(00)00147-5

Sarangi, A. G. A., & Parihar, D. K. S. S. S. (2016). Indian Journal of Hill Farming Evaluation of Methods for Estimation of Reference Evapotranspiration, *29*(1), 79–86.

Singh, V. K., Satpathy, R., Parveen, R., & Jeyaseelan, A. P. T. (2010). Spatial Variation of Vegetation Moisture Mapping Using Advanced Spaceborne Thermal Emission & Reflection Radiometer (ASTER) Data. *Journal of Environmental Protection*, *1*(4), 448–455. https://doi.org/10.4236/jep.2010.14052

Stathopoulou, M., & Cartalis, C. (2007). Daytime urban heat islands from Landsat ETM+ and Corine land cover data: An application to major cities in Greece. *Solar Energy*, *81*(3), 358–368. https://doi.org/10.1016/j.solener.2006.06.014

Subedi, A., & Chávez, J. L. (2015). Crop Evapotranspiration (ET) Estimation Models: A Review and Discussion of the Applicability and Limitations of ET Methods. *Journal of Agricultural Science*, *7*(6), 50–68. https://doi.org/10.5539/jas.v7n6p50

Tabari, H., & Grismer, M. E. (2013). Comparative analysis of 31 reference evapotranspiration methods under humid conditions, 107–117. https://doi.org/10.1007/s00271-011-0295-z

Tasumi, M., Trezza, R., Allen, R. G., & Wright, J. L. (2003). U.S. Validation Tests on the SEBAL Model for

Evapotranspiration via Satellite, 1–14.

Tizikara, C., George, L., & Lugor, L. (2015). Post-conflict Development of Agriculture in South Sudan : Perspective on Approaches to Capacity Strengthening. https://doi.org/https://europa.eu/capacity4dev/sorudev/document/post-conflict-development-agriculture-south-sudan-approaches-capacity-strengthening

Trajkovic, S. (2005). Temperature-Based Approaches for Estimating Reference Evapotranspiration. *Journal of Irrigation and Drainage Engineering*, *131*(August), 316–323. https://doi.org/10.1061/(ASCE)0733-9437(2005)131:4(316)

Trajkovic, S. (2007). Hargreaves versus Penman-Monteith, *133*(February), 38–42.

Tran, V. D., & Pinon, *Æ*. A. (2009). Using remote sensing to evaluate the spatial variability of evapotranspiration and crop coefficient in the lower Rio Grande Valley , New Mexico, 93–100. https://doi.org/10.1007/s00271-009-0178-8

Tsouni, A., Kontoes, C., Koutsoyiannis, D., Elias, P., Mamassis, N., Sensing, R., … Penteli, P. (2008). Estimation of Actual Evapotranspiration by Remote Sensing: Application in Thessaly Plain, Greece, 3586–3600. https://doi.org/10.3390/s8063586

Valipour, M. (2015). Temperature analysis of reference evapotranspiration models. *Meteorological Applications*, *22*(3), 385–394. https://doi.org/10.1002/met.1465

Wagner, S. (2008). *Water balance in a poorly gauged basin in West Africa using atmospheric modelling and remote sensing information*. *Mitteilungen / Institut für Wasserbau, Universität Stuttgart* (Vol. 173). Retrieved from http://elib.uni-stuttgart.de/opus/volltexte/2008/3615/

Wagner, S., Kunstmann, H., Bárdossy, A., Conrad, C., & Colditz, R. R. (2009). Water balance estimation of a poorly gauged catchment in West Africa using dynamically downscaled meteorological fields and remote sensing information. *Physics and Chemistry of the Earth*, *34*(4–5), 225–235. https://doi.org/10.1016/j.pce.2008.04.002

NCEP Website: https://globalweather.tamu.edu/.

USGS Website: https://earthexplorer.usgs.gov/.

USGS Website: https://landsat.usgs.gov/using-usgs-landsat-8-product.

Weligepolage, K. (2005). ESTIMATION OF SPATIAL AND TEMPORAL DISTRIBUTION OF EVAPOTRANSPIRATION BY SATELLITE REMOTE SENSING A case study in Hupselse Beek , The Netherlands.

Weng, Q., Lu, D., & Schubring, J. (2004). Estimation of land surface temperature – vegetation abundance relationship for urban heat island studies, *89*, 467–483. https://doi.org/10.1016/j.rse.2003.11.005

Wikipedia. (n.d.). https://en.wikipedia.org/wiki/Roorkee.

Wisser, D., Frolking, S., Douglas, E. M., Fekete, B. M., Vörösmarty, C. J., & Schumann, A. H. (2008). Global irrigation water demand: Variability and uncertainties arising from agricultural and climate data sets. *Geophysical Research Letters*, *35*(24). https://doi.org/10.1029/2008GL035296

Yang, X., Zhou, Q., & Melville, M. (1997). Estimating local sugarcane evapotranspiration using landsat TM image and a VITT concept. *International Journal of Remote Sensing*, *18*(2), 453–459. https://doi.org/10.1080/014311697219196

Zheng, X., & Zhu, J. (2015). Temperature-based approaches for estimating monthly reference evapotranspiration based on MODIS data over North China. *Theoretical and Applied Climatology*, *121*(3–4), 695–711. https://doi.org/10.1007/s00704-014-1269-x